Increasing dependence of lowland population on mountain water resources

Daniel Viviroli[1,*], Matti Kummu[2], Michel Meybeck[3], Yoshihide Wada[4,5]

[1] Department of Geography, University of Zürich, Switzerland
[2] Water & Development Research Group, Aalto University, Espoo, Finland
[3] Université Pierre et Marie Curie, Paris, France
[4] International Institute for Applied Systems Analysis, Laxenburg, Austria
[5] Department of Physical Geography, Faculty of Geosciences, Utrecht University, The Netherlands

*** Corresponding author:**
Daniel Viviroli (daniel.viviroli@geo.uzh.ch)
Hydrology and Climate, Department of Geography, University of Zürich
Winterthurerstr. 190, CH-8057 Zürich, Switzerland

Keywords:
global water resources, climate change, global change, highland-lowland-systems, food security, irrigated areas, water towers, mountain areas

Mountain areas provide disproportionally high runoff in many parts of the world, but their importance for lowland water resources and food production has not been clarified so far. Here we quantify for the first time the extent to which lowland inhabitants potentially depend on runoff contributions from mountain areas (39% of land mass). We show that ~1.4 billion people (23% of world's lowland population) are projected to depend critically on runoff contributions from mountains by mid-21st century under a 'middle of the road' scenario, compared to ~0.2 B (8%) in the 1960s. This striking rise is mainly due to increased local water consumption in the lowlands, whereas changes in mountain and lowland runoff play a minor role only. We furthermore show that one third of global lowland area equipped for irrigation is currently located in regions that both depend heavily on runoff contributions from mountains and make unsustainable use of local blue water resources, a figure that is likely to rise to well over 50% in the coming decades. Our findings imply that mountain areas should receive particular attention in water resources management and underscore the protection they deserve in efforts towards sustainable development.

Water is a key resource for the 21st century: Mainly due to population growth and associated food production, global water consumption has increased almost four-fold over the past 100 years[1] and water demand is approaching the total renewable freshwater available today[2]. The importance of water for environmental, economic and social aspects places it at the heart of the UN Sustainable Development Goals (SDGs)[3]. Mountain areas, in turn, play an important role in water resources in that they often deliver disproportionally high runoff to the subjacent lowlands that is crucial for irrigation, industry, drinking, domestic use, hydropower and ecosystems[4–7]. In this context of superior runoff contributions, "mountain area" and "mountains" are used here in a broad definition that also includes hills and elevated plateaux[4,5] (Methods).

Because of their importance in water resources, the contributions of mountain areas need to be understood much better yet. In particular, demographic, socio-economic and environmental changes affecting mountain water resources must be viewed in the larger picture of global development planning and policy making[8]. The large lead times required for implementing adaptation measures, such as reservoirs and water transfer systems, emphasise the urgency of a solid basis for long-term management of water resources originating in mountain areas[9]. Moreover, sharpening the picture of increasing pressure imposed on mountain areas through rapidly growing water demand both in mountains and lowlands is a key ingredient to sustainable mountain development[10].

The importance of mountain areas in providing freshwater for a significant portion of the world population has been recognised in its principle for a long time[4,11], and a global typology of mountain areas in water resources revealed that almost half of these areas world-wide provide supportive or even essential water resources for the areas downstream[5]. In studies focused on individual regions, Asia has received particular attention due to the vast population of well over a billion that live in the river basins originating in High Mountain Asia[12,13].

Still lacking to date is a global overview that addresses and differentiates the potential dependence of lowland populations on mountain runoff, is meaningful at the regional scale, and assesses changes over time, including anticipated future changes[14,15]. In an attempt to fill this gap, we here present the first comprehensive mapping and quantification of lowland inhabitants depending on mountain water resources, and a subsequent analysis of the importance of mountain runoff contributions for food production. We achieve a resolution of 5' (arc minutes, ~9 km at the Equator) and can thus also examine smaller highland-lowland systems that would be clustered in the currently still common resolution of 30'. This improved resolution is also important for water resources management at the level of individual regions, as well as setting priorities in future research, especially for regions that do not dispose of detailed models and studies[15]. In the temporal dimension, we cover the time from 1961 to the present and consider three possible developments for runoff and consumptive water use until 2050. We explore a "middle of the road" scenario (SSP2-RCP6.0 pathway), a "green road" scenario (sustainability, accelerated demographic transition; SSP1-RCP4.5), and a "rocky road" scenario (regional rivalry, high population growth in developing countries; SSP3-RCP6.0). While the extension into the future is crucial for a more comprehensive planning of water resources under climate and global change, the look back allows for a quantification of changes in the Anthropocene era[16].

Dependence of lowland inhabitants on mountain water resources

Our assessment is based on a high-resolution and state-of-the-art Global Hydrological Model (GHM) that simulates both runoff as well as consumptive water use and includes reservoir regulation[17,18]. The model has already been applied to numerous projects that quantified global water resources and climate change impacts[17]. Based on relief roughness and elevation, the global land surface area (not including Greenland and Antarctica) is then divided into a mountain (39% of total) and a lowland (61%) part (Methods; Supplementary Fig. S1). The mountain part encompasses mountainous areas in the strict sense as well as plateaux and rugged hills of at least medium elevation. This is important because all of these areas can have an important role in providing runoff to the lowlands[5]. The extent of this importance largely depends on the combination of climatic conditions found in the mountain and lowland portions of a catchment[5,19]. Lowlands encompass the remaining land surface area.

We identify the potential dependence of lowland areas on mountain water resources by computing a water balance for each lowland raster cell, with local runoff on the credit side, and local consumptive water use and ecological flow requirements on the debit side. The resulting surplus or deficit of each lowland raster cell is then compared with a similar balance that represents average conditions in the related mountain area. 'Related' here means that this comparison always takes place in a river catchment, and thus follows the hydrological link between mountain and lowland areas (Fig. 1a). With the result of this balance, the dependence of each lowland raster cell on mountain runoff is determined, differentiating the potential contribution from mountains into essential, supportive, minor and negligible (Fig. 1b). Lowland areas depending on essential mountain surpluses are further analysed by assessing how large the mountain surplus is as compared to the lowland deficit. This allows for differentiating lowland regions where mountain surpluses are insufficient or even vastly insufficient for balancing out water deficits, and sensitivity towards variations and changes in the contribution from mountains is large. On this basis, we can then quantify the number of lowland people potentially depending on mountain runoff. A key benefit of this analysis is that we take into account local climatic conditions and water consumption patterns in the lowlands and thus can assess what portion of lowland population depends critically on mountain surpluses and where it is located. This issue was e.g. touched upon (but not elaborated in more detail) for the rivers that originate in High Mountain Asia[20]. A similarly differentiated picture will be painted for the dependence of lowland food production on mountain runoff.

Changes in the global picture from past over present to future

Results for the entire globe (excluding Greenland and Antarctica) in a decadal timeline from 1961 to 2050 reveal notable changes (Fig. 2a): The lowland population depending on essential mountain runoff contributions grows from ~0.6 B (23% of total lowland population) in the 1960s to ~1.8 B (38%) in the 2000s and ~2.5 B (39%) in the 2040s under the SSP2-RCP6.0 scenario (SSP1-RCP4.5: ~2.3 B / 38%; SSP3-RCP6.0: ~2.7 B / 40%). In relative terms, the major part of this growth took place in 1961–2010 already (Supplementary Fig. S2a), while dependence on contributions from mountains becomes increasingly critical, with ~0.2 B (8%) of population

benefiting from essential but insufficient contributions in the 1960s, ~0.8 B (17%) in the 2000s, and a projected ~1.4 B (23%) in the 2040s under SSP2-RCP6.0 (SSP1-RCP4.5: ~1.2 B / 21%; SSP3-RCP6.0: ~1.5 B / 23%). A complete lack of runoff surplus from mountain areas is found in various regions, caused by low runoff (e.g., parts of the Rocky Mountains and South Africa), high water consumption (e.g., parts of China and India), or both (e.g., parts of the Yellow River catchment) (Supplementary Fig. S3a, c, e). In the lowlands, such a lack is especially grave if a deficit prevails there (Supplementary Fig. S3b, d, f). In this case, the lowlands must be expected to resort to other options[21], including dams, desalination, water recycling, use of fossil groundwater and interbasin transfers (such as in California and China)[22]. Our analysis suggests that a number of catchments have already moved into this situation in the past decades or will do so until mid-21st century (e.g., on the Indian Peninsula[23]) (Supplementary Fig. S4, Supplementary Tables S1, S2).

These figures, however, only paint part of the picture since the dependence of lowland inhabitants on mountain runoff strongly depends on the climate zone in focus, and global averages thus tend to underrate this dependence in individual regions. Especially in dryer climate zones, mountains provide important runoff that is distributed downstream via the river systems[19]. In these cases, mountains are elevated humid islands within an arid region and thus match the original concept of "water towers"[5]. Therefore, we further analyse our results by hydrobelts, i.e. hydrological basins aggregated to regions with similar hydroclimatic characteristics[24] (Methods) (Figs. 2b–i, Supplementary Figs. S2b–i). The most notable changes are found in the North mid-latitude hydrobelt, where the lowland population depending on essential mountain contributions increases by almost a billion from ~0.4 B (26% of this hydrobelt's lowland population; 16% of world total lowland population) to ~1.4 B (45%; 22%) in the same time (Fig. 2c). Further notable increases are found in the North dry, North subtropical, Boreal and Equator hydrobelts (Fig. 2d, e, b, f).

Hot spot regions

The global picture shows a number of 'hot spot' regions where the dependence of lowlands on mountain runoff was high already in the past, is today or is projected to become so in the future (Fig. 3a–c, Box 1). South and East Asia are of particular relevance, especially the Ganges-Brahmaputra-Meghna catchment that hosts the largest number of lowland people depending on essential mountain contributions, namely 94 M in 1961–1970, 391 M in 2001–2010 and 570 M in 2041–2050 under SSP2-RCP6.0 (Table 1). It is worth noting that this six-fold increase (+476 M) also represents the major part of population growth in this catchment from 1961 to 2050 (+639 M). Another vast growth of lowland population depending on mountain contributions is found in the Yangtze River catchment, with a 2.6 fold increase from 114 M (1961–1970) over 263 M (2001–2010) to 293 M (2041–2050, SSP2-RCP6.0). Significant growth in lowland population (increase of more than 25 M from 1961–1970 to 2041–2050) in areas with essential mountain contributions is further found in the Nile and Niger River catchments, and it takes place even almost exclusively in these areas in the Amur, Kaveri, Euphrates-Tigris, Godavari, Indus, Pearl, and Volga River basins. At the level of countries, India shows the biggest increase in lowland population depending on essential mountain contributions (+646 M from 1961–1970 to 2041–2050, SSP2-RCP6.0), followed by China (+244 M), Pakistan (+152 M) and Egypt (+86 M) (Supplementary Table S3). In addition, many catchments have a notable lowland population that benefits from supportive runoff from mountain areas (Supplementary Table S4).

Main drivers for change

An important question for water resources management is whether the developments found here are driven by changes in runoff or by changes in water consumption[25]. Since we are interested in a comparison of lowland and mountain water balance, it is imperative to examine the relation of mountain runoff to lowland runoff over time. However, no fundamental changes in pattern are found in this relation (Supplementary Fig. S6), although it changes in favour mountain runoff in some regions (e.g., Himalayas, parts of the Andes) and in favour of lowland runoff in others (e.g., Central and Southern Rocky Mountains, South-West Africa, Atlas Mountains). Moderate changes are also visible in a breakdown to individual hydrobelts (Supplementary Fig. S7b–i), but do not prevail in the global summary (Supplementary Fig. S7a).

We achieve a deeper insight into the drivers by looking at the number of people projected to reside in a specific dependence category 2041–2050, and comparing that to results from a baseline scenario with runoff and total water consumption unchanged at 1961–1970 values. There are then four potentially relevant drivers: mountain runoff, mountain water consumption, lowland runoff, and lowland water consumption. Varying one of these at a time shows that the 2.5-fold increase in lowland water consumption between 1961 and 2050 (SSP2-RCP6.0) is by far the most important factor shifting people towards higher dependency on mountain runoff (Table 2). At global scale, per capita lowland water consumption does not exhibit major changes from 1961 to 2050 under all

scenarios considered, although there are regions with clear increase (e.g. Boreal and North mid-latitude hydrobelts) and decrease (e.g., North dry and Equator hydrobelts). Overall, lowland population development is therefore the most important factor in determining the dependence of lowlands on mountain runoff (Supplementary Fig. S8), whereas changes in mountain population, mountain runoff and lowland runoff are of minor importance.

Potential impacts on food production

Roughly, three quarters of global food production (caloric value) originate in lowlands today, and lowlands host about the same share of global area equipped for irrigation (AEI) (Supplementary Tables S5, S6). Mountain areas, despite their small share in food production, can contribute important runoff to lowland irrigated agriculture[26] (Fig. 4): Of the AEI present in lowlands 2001–2010, 68% (or $1.54 \cdot 10^6$ km^2) were located in regions that depend on essential runoff contributions from the mountains. Half of that ($0.77 \cdot 10^6$ km^2) show low sustainability of local blue water use (liquid water in rivers, lakes, and aquifers[27]) in addition, thus amplifying the dependence on contributions from mountain areas.

Under runoff and water consumption conditions projected for 2041–2050 (SSP2-RCP6.0), as much as 56% of lowland AEI ($1.28 \cdot 10^6$ km^2) would be located in regions both depending on mountain runoff and making unsustainable use of local blue water resources. This expansion is mainly occurring in regions that did already depend on mountain water resources 2001–2010, while the area making unsustainable use of blue water resources also increases. The North dry hydrobelt, already under critical conditions to a large extent in the 1960s and 2000s, shows a particularly alarming development in this direction, with 86% of lowland AEI projected to be under unsustainable conditions and depending on mountain areas. An important rise in this combination of critical conditions is also apparent in the North subtropical hydrobelt. Overall, these numbers imply that mountain areas could become even more important to support food production in the future, especially in regions like India, Egypt, and Southern Africa (Supplementary Fig. S9).

Implications for global water resources

Our new findings provide a guide to regions where more profound knowledge is necessary regarding the dependence of lowlands on mountain runoff, and the impacts of population dynamics and climatic changes should be studied in more detail. For facilitating water resources management, it will be imperative to also consider the seasonality of both lowland water consumption and mountain water provisions, especially with a view to changes in the important contribution of snowmelt and, in some regions, also ice melt[28–32]. Bearing in mind the sensitivity of mountain environments, the amplification of warming with elevation and the non-linear reaction of the cryosphere to climate forcing[33–36], these changes in seasonality may also reveal a more distinct impact of climate change and qualify the dominant control of lowland water consumption found in this study, especially in wet-dry climates of the subtropics.

We show that lowland water resources have become increasingly dependent on mountain areas in the past decades and are likely to become even more so in the future: Water scarcity is projected to be more severe, and ongoing groundwater depletion may pose a serious water security risk in intense agricultural regions[2,12]. This might cause higher vulnerability under an uncertain climate[36], as highlighted by our finding that well over half of lowland areas equipped for irrigation might depend both on mountain water surpluses and unsustainable lowland water resources by mid-21st century under a ‘middle of the road‘ scenario. At the same time, population and land use pressure are expected to increase further[36,37], leading to considerable challenges to environmental sustainability[38]. In addition, large-scale human interventions like land use and land cover changes, construction of dams and reservoirs as well as withdrawals from surface water and groundwater negatively affect the downstream parts of river catchments and may lead to additional imbalances between mountain and lowland areas[39]. All of this underscores the special protection and attention mountain areas deserve in efforts towards sustainable development, and suggests that highland-lowland interactions should not be a one-way process in favour of the lowlands, but that compensation mechanisms in the reverse direction should be considered to support sustainable development both in mountain and lowland areas[26]. In summary, our work emphasises that hydrosolidarity[40] between mountain and lowland populations sharing a common river basin is essential, with the goal of an ethically sound orchestration of land, water and ecosystem related activities.

Acknowledgements
Part of this study was funded by a SNSF Fellowship for advanced researchers to DV (grant no. PA00P2_131464). MK was funded by Academy of Finland funded projects SCART (grant no. 267463) and WASCO (grant no. 305471), Emil Aaltonen Foundation funded project 'eat-less-water', and Academy of Finland SRC project 'Winland'. For their roles in producing, coordinating, and making available the ISI-MIP model output, we acknowledge the modelling groups (see Methods) and the ISI-MIP coordination team.

Author Contributions
DV designed the research together with all co-authors; MM initiated some of the global scale river basin typologies used in this paper; DV performed the main research; MK contributed ecological flow, food production and irrigation analyses and implemented delta change method; YW performed global hydrological model runs and contributed data on sustainability of blue water use; DV interpreted the results and wrote the paper with all co-authors providing comments.

Additional information
See Supplementary material.

Competing Financial Interests
We declare no competing financial interests.

References
1. Kummu, M. *et al.* The world's road to water scarcity: shortage and stress in the 20th century and pathways towards sustainability. *Sci. Rep.* **6,** 38495; 10.1038/srep38495 (2016).
2. Wada, Y. *et al.* Modeling global water use for the 21st century: the Water Futures and Solutions (WFaS) initiative and its approaches. *Geosci. Model Dev.* **9,** 175–222; 10.5194/gmd-9-175-2016 (2016).
3. United Nations General Assembly (UNGA). *Transforming our world: the 2030 Agenda for Sustainable Development.* Resolution adopted by the General Assembly on 25 September 2015 (2015).
4. Bandyopadhyay, J., Kraemer, D., Kattelmann, R. & Kundzewicz, Z. W. in *Mountains of the World,* edited by B. Messerli & J. D. Ives (Parthenon, New York, NY, London, 1997), pp. 131–155.
5. Viviroli, D., Dürr, H. H., Messerli, B., Meybeck, M. & Weingartner, R. Mountains of the world, water towers for humanity: Typology, mapping, and global significance. *Water Resour. Res.* **43,** W07447; 10.1029/2006WR005653 (2007).
6. Green, P. A. *et al.* Freshwater ecosystem services supporting humans. Pivoting from water crisis to water solutions. *Global Environ. Chang.* **34,** 108–118; 10.1016/j.gloenvcha.2015.06.007 (2015).
7. Debarbieux, B. & Price, M. F. Representing mountains: from local and national to global common good. *Geopolitics* **13,** 148–168; 10.1080/14650040701783375 (2008).
8. Wohl, E. E. *Disconnected Rivers. Linking rivers to landscapes* (Yale University Press, New Haven, CT, 2004).
9. Bach, A. W. & Price, L. W. in *Mountain Geography,* edited by M. F. Price, A. C. Byers, D. A. Friend, T. Kohler & L. W. Price (University of California Press, Oakland, CA, 2013), pp. 41–84.
10. Wehrli, A. Why mountains matter for sustainable development. Switzerland's new mountain program in development cooperation. *Mt. Res. Dev.* **34,** 405–409; 10.1659/MRD-JOURNAL-D-14-00096.1 (2014).
11. Kundzewicz, Z. W. & Kraemer, D. in *Ecohydrology of High Mountain Areas: Proceedings of the International Conference on Ecohydrology of High Mountain Areas, Kathmandu, Nepal, 24–28 March 1996,* edited by S. R. Chalise, *et al.* (Kathmandu, 1998), pp. 175–185.
12. Immerzeel, W. W., van Beek, L. P. H. & Bierkens, M. F. P. Climate change will affect the Asian water towers. *Science* **328,** 1382–1385; 10.1126/science.1183188 (2010).
13. United Nations World Water Assessment Programme (WWAP) (ed.). *The United Nations World Water Development Report 3: Water in a Changing World* (UNESCO and Earthscan, Paris, London, 2009).
14. Adam, J. C., Hamlet, A. F. & Lettenmaier, D. P. Implications of global climate change for snowmelt hydrology in the twenty-first century. *Hydrol. Process.* **23,** 962–972; 10.1002/hyp.7201 (2009).
15. Viviroli, D. *et al.* Climate change and mountain water resources: overview and recommendations for research, management and policy. *Hydrol. Earth Syst. Sci.* **15,** 471–504; 10.5194/hess-15-471-2011 (2011).
16. Crutzen, P. J. Geology of mankind. *Nature* **415,** 23; 10.1038/415023a (2002).

17. Wada, Y., Wisser, D. & Bierkens, M. F. P. Global modeling of withdrawal, allocation and consumptive use of surface water and groundwater resources. *Earth Syst. Dynam.* **5,** 15–40; 10.5194/esd-5-15-2014 (2014).
18. Sutanudjaja, E. H. *et al.* PCR-GLOBWB 2: a 5 arcmin global hydrological and water resources model. *Geosci. Model Dev.* **11,** 2429–2453; 10.5194/gmd-11-2429-2018 (2018).
19. Viviroli, D., Weingartner, R. & Messerli, B. Assessing the hydrological significance of the world's mountains. *Mt. Res. Dev.* **23,** 32–40; 10.1659/0276-4741(2003)023[0032:ATHSOT]2.0.CO;2 (2003).
20. Immerzeel, W. W. & Bierkens, M. F. P. Asia's water balance. *Nat. Geosci.* **5,** 841–842; 10.1038/ngeo1643 (2012).
21. Wada, Y., Gleeson, T. & Esnault, L. Wedge approach to water stress. *Nat. Geosci.* **7,** 615–617; 10.1038/ngeo2241 (2014).
22. Ghassemi, F. & White, I. *Inter-Basin Water Transfer. Case studies from Australia, United States, Canada, China, and India* (Cambridge University Press, New York, NY, 2007).
23. Misra, A. K. *et al.* Proposed river-linking project of India. A boon or bane to nature. *Environ. Geol.* **51,** 1361–1376; 10.1007/s00254-006-0434-7 (2007).
24. Meybeck, M., Kummu, M. & Dürr, H. H. Global hydrobelts and hydroregions: improved reporting scale for water-related issues? *Hydrol. Earth Syst. Sci.* **17,** 1093–1111; 10.5194/hess-17-1093-2013 (2013).
25. Vörösmarty, C. J., Green, P. A., Salisbury, J. & Lammers, R. B. Global water resources: vulnerability from climate change and population growth. *Science* **289,** 284–288; 10.1126/science.289.5477.284 (2000).
26. Messerli, B. Global change and the World's mountains. Where are we coming from, and where are we going to? *Mt. Res. Dev.* **32,** S55–S63; 10.1659/MRD-JOURNAL-D-11-00118.S1 (2012).
27. Falkenmark, M. & Rockström, J. The new blue and green water paradigm: Breaking new ground for water resources planning and management. *J. Water Res. Pl. ASCE* **132,** 129–132 (2006).
28. Barnett, T. P., Adam, J. C. & Lettenmaier, D. P. Potential impacts of a warming climate on water availability in snow-dominated regions. *Nature* **438,** 303–309; 10.1038/nature04141 (2005).
29. Mankin, J. S., Viviroli, D., Singh, D., Hoekstra, A. Y. & Diffenbaugh, N. S. The potential for snow to supply human water demand in the present and future. *Environ. Res. Lett.* **10,** 114016; 10.1088/1748-9326/10/11/114016 (2015).
30. Stewart, I. T. Changes in snowpack and snowmelt runoff for key mountain regions. *Hydrol. Process.* **23,** 78–94; 10.1002/hyp.7128 (2009).
31. Huss, M. *et al.* Toward mountains without permanent snow and ice. *Earth's Future* **5,** 418–435; 10.1002/2016EF000514 (2017).
32. Salzmann, N., Huggel, C., Rohrer, M. & Stoffel, M. Data and knowledge gaps in glacier, snow and related runoff research – A climate change adaptation perspective. *J. Hydrol.* **518,** 225–234; 10.1016/j.jhydrol.2014.05.058 (2014).
33. Pepin, N. C. *et al.* Elevation-dependent warming in mountain regions of the world. *Nat. Clim. Chang.* **5,** 424–430; 10.1038/nclimate2563 (2015).
34. Barry, R. G. *Mountain weather and climate.* 3rd ed. (Cambridge University Press, Cambridge, New York, NY, 2008).
35. Beniston, M. Mountain weather and climate: A general overview and a focus on climatic change in the Alps. *Hydrobiologia* **562,** 3–16; 10.1007/s10750-005-1802-0 (2006).
36. Messerli, B., Viviroli, D. & Weingartner, R. Mountains of the world: vulnerable water towers for the 21st century. *Ambio Special Report,* 29–34 (2004).
37. Kummu, M. *et al.* Over the hills and further away from coast. Global geospatial patterns of human and environment over the 20th–21st centuries. *Environ. Res. Lett.* **11,** 34010; 10.1088/1748-9326/11/3/034010 (2016).
38. Grover, V. I., Borsdorf, A., Breuste, J., Tiwari, P. C. & Frangetto, F. W. *Impact of global changes on mountains. Responses and adaptation* (CRC Press, Boca Raton, FL, 2014).
39. Veldkamp, T. I. E., Wada, Y., Aerts, J C J H & Ward, P. J. Towards a global water scarcity risk assessment framework. Incorporation of probability distributions and hydro-climatic variability. *Environ. Res. Lett.* **11,** 24006; 10.1088/1748-9326/11/2/024006 (2016).
40. Falkenmark, M. Forward to the Future: A Conceptual Framework for Water Dependence. *Ambio* **28,** 356–361 (1999).
41. Körner, C. *et al.* A global inventory of mountains for bio-geographical applications. *Alp Botany* **127,** 1–15; 10.1007/s00035-016-0182-6 (2017).

Boxes

Box 1. Potential dependence of lowlands on mountain water resources in selected river basins.

In the **Indus River basin**, lowland population is projected to increase close to fivefold from 44 M in the 1960s to 210 M in the 2040s (SSP2). Even though per-capita lowland water consumption decreases by almost two thirds, nearly all lowland inhabitants (93–95%) depend on mountain runoff throughout 1961–2050, a large majority (80–85%) even on vastly insufficient mountain runoff. In addition, the immense irrigation system makes unsustainable use of local blue water resources and depends critically on mountain surpluses. Conflict potential over use of mountain runoff and vulnerability to changes are high.

The **Niger River basin** (without Benue River) shows a marked increase in dependent lowland population, from only 4% in the 1960s to a projected 40% in the 2040s (SSP2). Together with a sevenfold increase in lowland population 1961–2050 and low but stable lowland per-capita water consumption, this puts 73 M lowland inhabitants in dependency on mountain water resources by the 2040s.

In the lowlands of the **Nile River basin**, dependency on contributions from the two mountainous source areas is constantly high at 80–85% of population and concentrates on the lower parts and the delta area in Egypt, as well as on the South of Sudan. 21% of lowland population were dependent on vastly insufficient mountain surpluses in the 1960s, with a projected rise to 53% in the 2040s (SSP2). Projected lowland population growth 1961–2050 is more than fourfold and sets off a decrease in lowland per-capita water consumption of roughly 60%. Efforts to make more extensive use of water upstream in the Ethiopian Highlands (Blue Nile River) bear considerable conflict potential.

The **Yangtze River basin**'s mountain runoff is under high pressure of use, not only in the basin's lowlands where 263 M people (74% of lowland population) depend on it in the 2000s: Interbasin water transfers to the rivers further north compensate for absence of mountain surpluses in the **Yellow River basin** (projected to cease in the 2020s) and the **Hai He River basin** (missing from the 1960s onwards) that together had a lowland population of 141 M in the 2000s. The lowlands of all three river basins are characterised by high population density and extensive irrigated agriculture, and lowland per-capita water consumption is projected to rise strongly, especially in the Yellow and Hai He River basins where 1960s values are expected to roughly double by the 2040s.

In the **Colorado River basin** (US and Mexico), almost the entire lowland population (96–100%) depends on vastly insufficient mountain water resources throughout 1961–2050, even though lowland per-capita water consumption halves over this time. This critical dependence extends to irrigated agriculture that made unsustainable use of local blue water already in the 1960s, and is exacerbated by interbasin transfers to south-western California including Greater Los Angeles. These conditions foster disputes over water use between Mexico and the US, and even within the US, and render water users vulnerable to drought events.

Tables

Table 1. Lowland population depending on essential mountain runoff contributions 1961–2050. Details are shown for all river catchments with a lowland population of 10 M or more in 2041–2050 that potentially depend on essential mountain runoff contributions. The numbers are given in Million people and encompass all areas depending on contributions that are essential and sufficient (yellow), essential but insufficient (orange) and essential but vastly insufficient (red). Results refer to catchments with a share of mountain area in total area of at least 5%, projections are based on the SSP2-RCP6 scenario. Results for further hot spot regions mentioned in the main text but not appearing here are reported in Supplementary Table S2.

#	*River catchment*	*1961–1970*	*2001–2010*	*2041–2050*[a]	*Major mountain range(s), hills and plateau(x)*[b]	*Share of mountain area in total area*	*Hydrobelt*[c]
1	Ganges-Brahmaputra-Meghna	94.0	390.6	$570.4^{+20.7}_{-25.9}$	Himalayas, Mishmi Hills, Meghalaya Hills, Chin Hills	44%	NML
2	Chang Jiang (Yangtze)	114.3	263.4	$293.4^{+15.8}_{-4.7}$	Yunnan-Guizhou Plateau, Tibetan Plateau, Bayan Har Mountains, Shaluli Mountains	69%	NML
3	Indus	41.0	115.2	$200.5^{+3.4}_{-0.9}$	Himalayas, Hindu Kush, Sulaiman Range, Karakoram Range	69%	NML
4	Nile	32.9	87.0	$143.4^{+2.1}_{-0.6}$	Ethiopian Highlands[d], Albertine Rift Mountains[e], Nuba Mountains	33%	NDR
5	Niger[f]	0.9	18.5	$73.3^{+7.2}_{-18.5}$	Guinea Highlands, Fouta Djallon, Aïr massif	8%	NST
6	Godavari	5.5	42.0	$68.0^{+4.1}_{-3.7}$	Eastern Ghats, Western Ghats	22%	NST
7	Shatt Al-Arab (Tigris, Euphrates)	8.8	30.1	$63.9^{+2.8}_{-5.0}$	Zagros Mountains, Taurus Mountains	41%	NDR
8	Amur	20.1	45.2	$49.0^{+0.7}_{-1.0}$	Yablonovy Range, Greater Khingan Range, Lesser Khingan Range, Sikhote-Alin	60%	BOR
9	Volga	14.3	38.9	$43.3^{+0.7}_{-1.5}$	Ural Mountains	5%	NML
10	Zhujiang (Pearl)-Xi Jiang (West)-Bei Jiang (North)-Dong Jiang (East)	1.8	2.6	$36.5^{+15.1}_{-1.5}$	Yunnan-Guizhou Plateau, Nanling Mountains	73%	NST
11	Kaveri	4.0	22.4	$34.9^{+0.0}_{-1.4}$	Western Ghats, Eastern Ghats	52%	NST
12	Tapti[g]	1.3	11.3	$25.6^{+0.3}_{-7.1}$	Satpura Range, Western Ghats	28%	NST
13	Chao Phraya	5.2	18.5	$22.3^{+0.8}_{-1.0}$	Phi Pan Nam Range, Shan Plateau, Luang Prabang, Range, Phetchabun Mountains	50%	NST
14	Mekong	1.6	12.2	$21.7^{+4.2}_{-0.5}$	Annamese Cordillera, Luang Prabang Range, Shan Plateau, Tanggula Mountains	54%	NST
15	Ob	10.4	18.3	$20.8^{+0.3}_{-0.5}$	Altai Mountains, Kuznetsky Alatau Mountains, Ural Mountains	16%	BOR

[continued on next page]

16	Amu Darya	3.8	12.6	$20.2^{+0.0}_{-0.0}$	Pamirs, Hindu Kush	69%	NDR
17	Han [Korea]-Imjin	0.0	16.8	$19.4^{+0.1}_{-0.2}$	T'aebaek Mountains, Sobaek Mountains	73%	NML
18	Narmada	0.7	9.7	$19.2^{+2.3}_{-2.9}$	Satpura Range, Vindhya Range	33%	NST
19	Danube	5.1	11.5	$18.3^{+1.1}_{-1.1}$	Carpathian Mountains, European Alps, Dinaric Alps, Balkan Mountains	52%	NML
20	Hong (Red)	0.0	9.5	$14.5^{+5.2}_{-0.7}$	Yunnan-Guizhou Plateau, Ailao Mountains, Hoang Lien Son Range, Song Ma Range	87%	NST
21	St. Lawrence	0.0	0.0	$13.2^{+0.9}_{-1.3}$	Superior Upland, Adirondack Mountains, Laurentian Mountains, Appalachian Mountains	9%	NML
22	Syr Darya	4.9	10.0	$12.9^{+0.1}_{-0.0}$	Tien Shan, Alai Range	52%	NDR
23	Mahanadi	0.8	9.7	$10.8^{+4.0}_{-4.8}$	Eastern Ghats, Chota Nagpur Plateau, Satpura Range	31%	NST
	Remaining catchments	*187.0*	*546.1*	$657.8^{+143.7}_{-80.5}$	-	*38%*	-
	Total	***558.4***	***1 763.4***	$\mathbf{2\,463.5^{+236.4}_{-185.0}}$	-	***39%***	-

[a] ensemble median for SSP2-RCP6.0, with differences to the ensemble minimum and maximum added in subscript and superscript, respectively

[b] following ref. [41] and area labels of major physiographic features provided by Natural Earth (version 3.0.0, available at http://www.naturalearthdata.com)

[c] BOR: Boreal; NML: North mid-latitude; NDR: North dry; NST: North subtropical (ref. [24])

[d] for the Blue Nile River

[e] for the White Nile River

[f] without the Benue River, which was separated from the Niger River because the paths of the two rivers follow climatically very different routes (Methods).

[g] For the Tapti River, one GCM ensemble member sees the entire lowland population receiving no more surplus from the mountains. This ensemble member was not used for computing the bounds shown here.

Table 2. Factors that drive changes in dependence on mountain water resources 2041–2050. As a baseline, it was assumed that runoff and total consumptive water use remain unchanged at 1961–1970 level. The impact of projected changes in mountain runoff, mountain water consumption, lowland runoff and lowland water consumption are then given below (all referring to SSP2-RCP6.0), noting the number of people (in millions) added or taken from each particular class of water resources index ***W*** by these changes (details in Supplementary Fig. S13).

	Essential, but vastly insufficient (red)	*Essential, but insufficient (orange)*	*Essential, and sufficient (yellow)*	*Supportive (green)*	*Minor (cyan)*	*Negligible (navy)*	*No surplus (gray)*
No changes in runoff and consumptive water use	**373**	**196**	**962**	**2 610**	**983**	**309**	**136**
Projected changes in mountain runoff	-26	+43	-16	-197	+36	+157	+3
Projected changes in mountain water consumption	-32	-17	-83	-231	+101	+92	+171
Projected changes in lowland runoff	+3	-18	+312	-223	-68	-7	0
Projected changes in lowland water consumption	+579	+259	+241	-574	-418	-87	0
All projected changes combined	**+521**	**+326**	**+86**	**-850**	**-337**	**-63**	**+316**

Figures

Figure 1. Analysis framework. For each raster cell in the lowlands, a water balance is computed, and for comparison, a similar average water balance is computed for the mountain area upstream in the same river basin (a). The dependence of the lowlands on mountain water resources is then assessed by comparing these two water balances (b) (Methods).

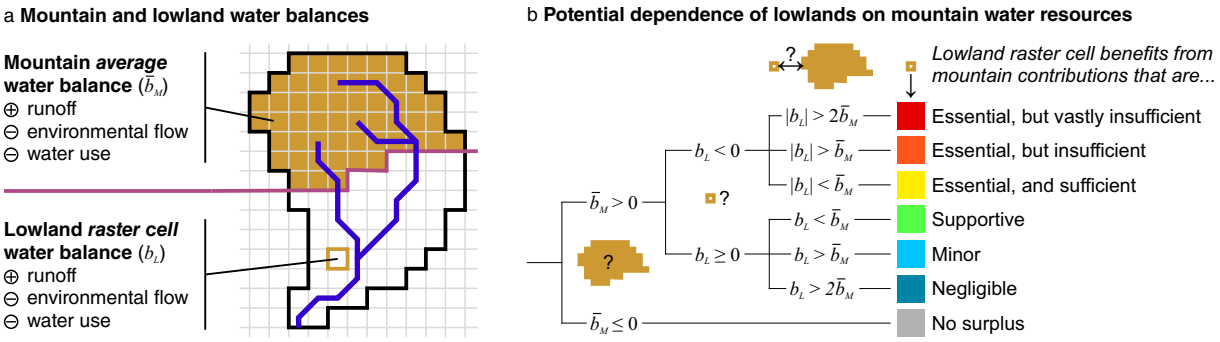

Figure 2. Dependence on mountain water resources 1961–2050. Results are shown as decadal averages for lowland population in each category, summarised for all hydrobelts (a) as well as differentiated by hydrobelt (b–i); hydrobelts are limited by river basin boundaries[24] (Methods). Corresponding fractions of lowland population are shown in Supplementary Fig. S2.

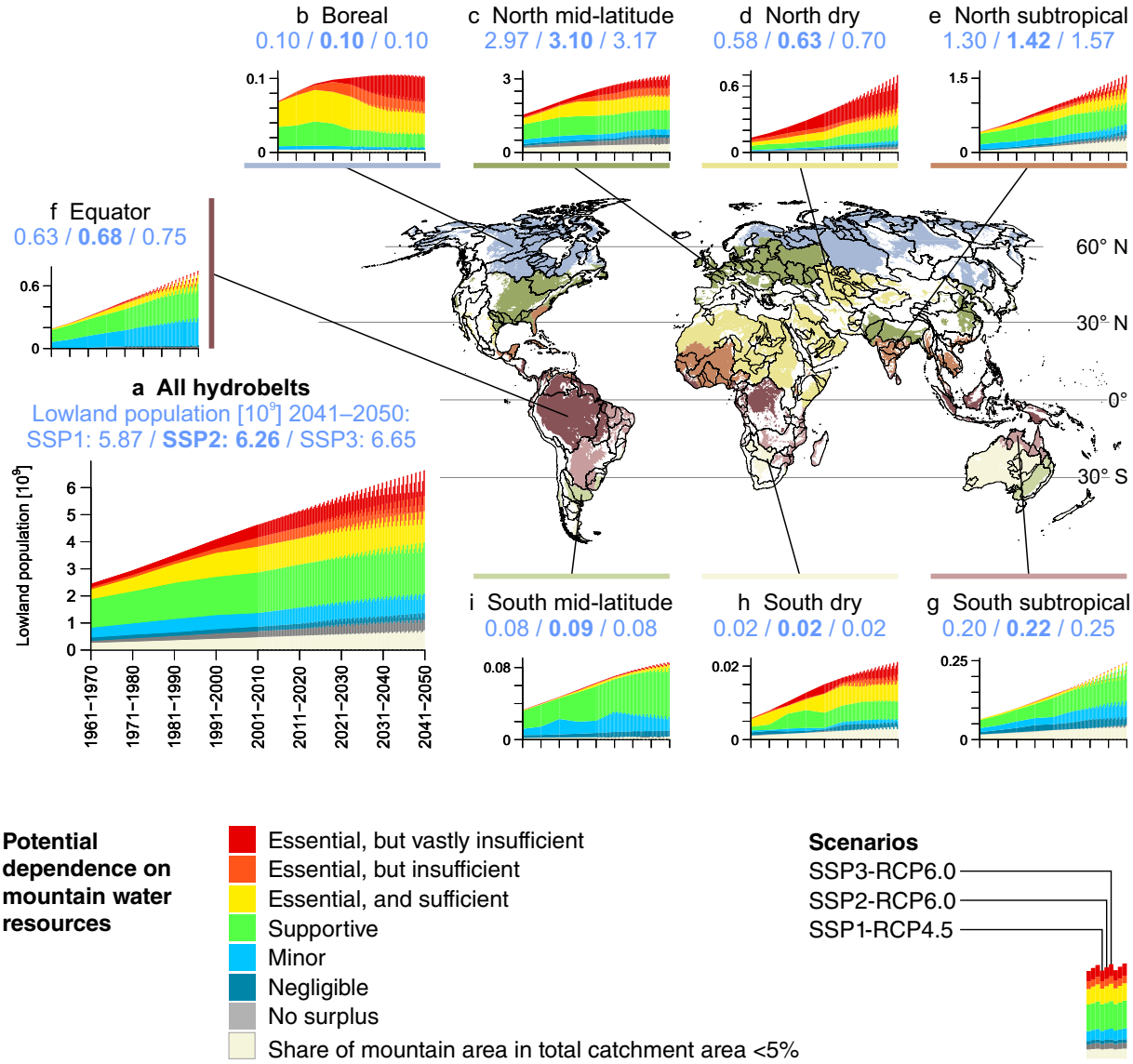

Figure 3. Spatial patterns in dependence on mountain water resources 1961–2050. The maps show water resources index ***W*** (Methods) for 1961–1970 (a), 2001–2010 (b), and 2041–2050 (SSP2-RCP6.0) (c). Beige denotes areas where mountains as per the definition used here occupy less than 5% of total catchment area, and an assessment of their contributing potential to lowland water resources should only be done carefully (shown in Supplementary Fig. S10). At the bottom, magnifications are shown for selected hot spot regions in 2041–2050 (d, e). These reveal population density in addition. Area equipped for irrigation and food production are shown in Supplementary Fig. S5. The boundaries of catchments with an area of 100 000 km² and more are drawn for orientation, and the locations of the example river basins presented in Box 1 are shown: 1) Colorado US/MEX, 2) Niger without Benue, 3) Nile, 4) Indus, 5) Yangtze.

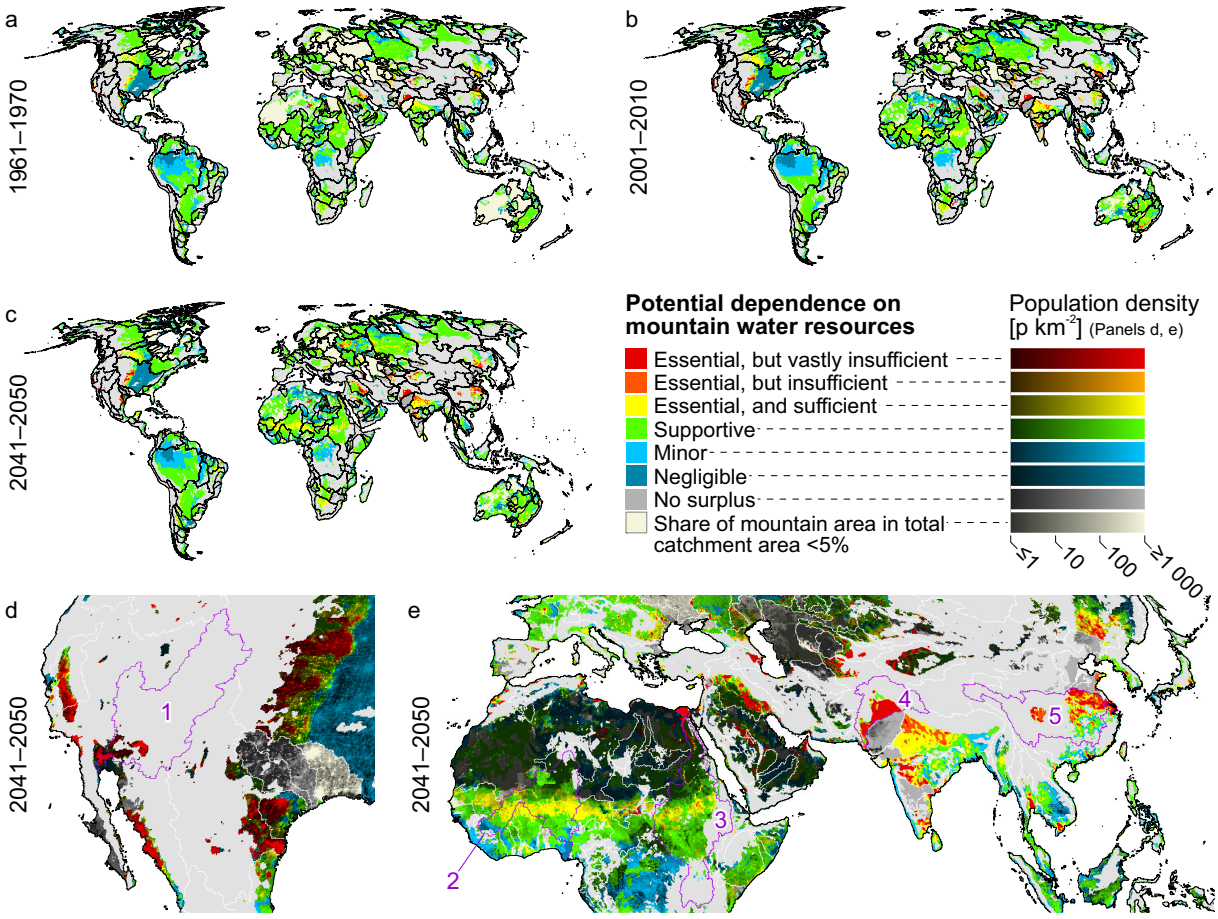

Figure 4. Lowland area equipped for irrigation (AEI) under non-sustainable blue water use and depending on essential mountain runoff contributions in the 1960s, 2000s and 2040s. Results are shown for hydrobelts (BOR: Boreal, NML: North mid-latitude, NDR: North dry, NST: North subtropical, EQT: Equatorial, SST: South subtropical, SDR: South dry; SML: South mid-latitude; for a map of hydrobelts see Fig. 2) and for the entire land surface area (ALL; without Greenland and Antarctica). Projections are based on the SSP2-RCP6 scenario.

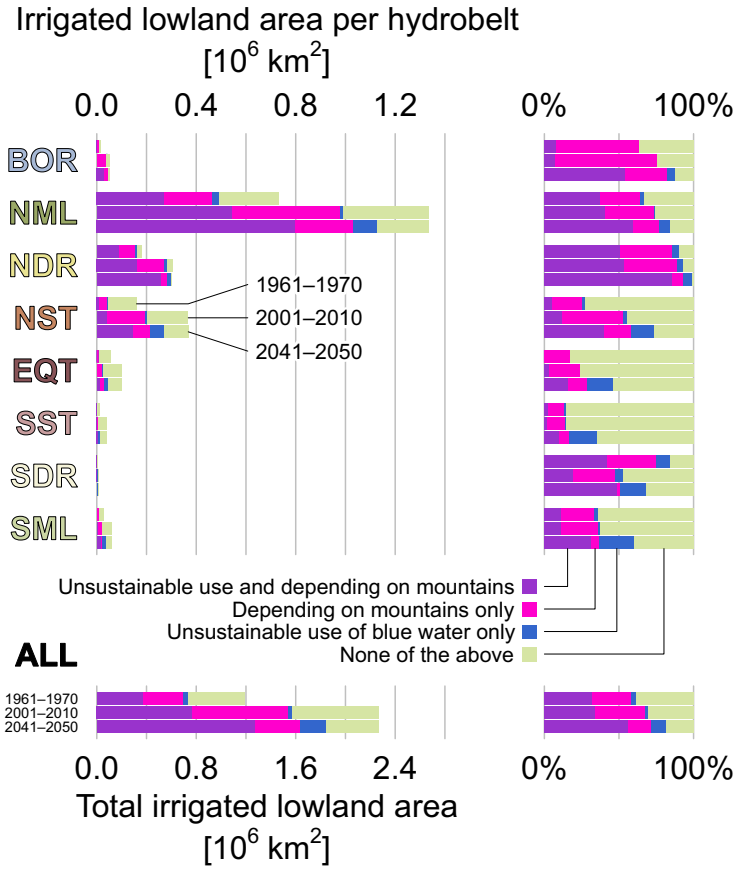

Methods

Catchments. We perform our analyses individually for each river catchment with an area of 10 000 km² or more. Smaller catchments are aggregated to groups contributing to the same coastal segment[1], and each of these groups is analysed individually as well. All results are then composited for a global map. This scheme follows the framework developed in ref. [2] whereas the original catchment boundaries and the coastal segmentation were refined from 30' (arc minutes, ~56 km at the Equator) to 5' (~9 km) resolution using high-resolution hydrographic information[3,4] and a detailed topographic atlas[5].

To establish a hydrological connection between large urban areas at the coast and major rivers nearby, the catchments of 48 rivers were extended to contain major delta areas[6]. Depending on the prevailing conditions, the main river catchment is thus extended by areas with high population and high runoff (e.g., Ganges-Brahmaputra-Meghna, Mississippi and Niger River Deltas), high population and low runoff (e.g., Indus, Nile and Yellow River Deltas), low population and high runoff (e.g., Amazon River Delta), as well as low population and low runoff (e.g., Lena and Mackenzie River Deltas). River systems are analysed jointly if they all contribute to the same delta area and, in addition, delta morphology and population distribution make it difficult to attribute the flow of the individual rivers to individual population centres. This is the case for the Ganges, Brahmaputra and Meghna Rivers (Bengal Delta), the Rhine, Meuse and Scheulte Rivers (Rhine Delta) and the Pearl, West, North and East Rivers (Pearl River Delta).

Due to a lack of reliable and comprehensive data, actual water transfers from one basin to another (interbasin transfers, e.g. from Yangtze River in northern direction) are not considered. For similar reasons, the hydrological link to irrigated areas situated outside of the supplying catchment is not established (relevant e.g. in the Nile River catchment). Both factors should be included in future studies with more regional focus, provided that suitable data become available.

We keep river network and thus catchment boundaries constant over time and do not consider the potential segmentation and shortening of rivers in dry regions that could result from reduced runoff (e.g., upper Niger River, White Nile River, Chari and Logone Rivers, Tarim River).

Mountain and lowland areas. We use "mountains" and "mountain areas" as extended geographic terms rather than in a strict geomorphologic sense. They encompass elevated terrain with potentially high relevance in water resources for the subjacent lowlands and refer to areas that are characterised with the symbolic term "water towers"[2,7]. Mountain areas have their counterpart in lowland areas, which are the areas that depend on mountain water resources, and are affected by environmental and societal change in mountain areas[8,9]. This follows earlier mountain-related studies on global change (e.g., refs. [10,11]) and water resources (e.g., refs. [2,12]), rooted in the physical and socioeconomic linkages between mountain and lowland areas. A related concept is that of "highland-lowland interactive systems" as examined in a United Nations University (UNU) programme initiated in 1978[13,14].

More specifically, our definition of mountain areas is based on a comprehensive typology of relief roughness and elevation. This typology, originally conceived at a resolution of 30' (see ref. [15] for details), was enhanced for our resolution of 5' on the basis of a high-resolution (7.5", arc seconds, ~0.23 km at the Equator) Digital Terrain Model (DTM)[16] (Supplementary Fig. S1). Following an earlier typology of global mountain water resources[2], we then chose a rather extensive definition that covers mountain areas of low, middle, high and very high elevation and also includes rugged hills as well as plateaux of medium, high and very high elevation. This is imperative because all of these relief classes can have an important role in providing runoff to lowland areas[2]. A further differentiation of results into relief types (as provided in ref. [2]) could reveal additional patterns but is beyond the scope of the present study, and not necessary for the overview envisaged here.

In detail, our definition of mountain areas includes (1) all areas above 200 m a.s.l. if their relief roughness (RR) is at least 45‰, (2) all areas above 500 m a.s.l. if RR is at least 21‰, (3) all areas above 1 000 m a.s.l. if RR is at least 10‰, and (4) all areas above 1 500 m a.s.l. regardless of RR. Criterion (3) is an addition to the original typology that was necessary to depict more realistically high-elevation lowland areas at our improved resolution, most of all in the Kalahari Desert and the Tarim Basin. It should be noted that this additional criterion might mix low-elevation regions (e.g., alluvial plains) with higher-elevation areas in some exorheic regions such as South Africa. The thresholds for RR were adapted from ref. [2] to reflect the relation between resolution of the detail DTM and that of the results in our study (7.5" to 5'), which slightly differs from the original relation (30" to

30'). To classify lakes in a way meaningful for our study, we assigned them the average RR of the raster cells along their outline and then classified them using above rules. This procedure was applied to all natural and dammed lakes with an area of at least 50 km^2, except for the Caspian Sea that was not considered part of the land mass. To achieve a more consistent delineation of mountain areas, single isolated mountain cells within lowland areas were eliminated by retaining the more frequent of the two classes in a moving window of 5×5 raster cells. As a result, 39% of global land surface area ($132.7 \cdot 10^6$ km^2, omitting Greenland and Antarctica, but including endorheic areas) is classified as mountains, the remaining area as lowlands. This re-creates the extent chosen in an earlier typology of mountains as "water towers"[2] and roughly compares to the figure of 36% of land area mentioned by ref. [17] as belonging to mountain and hilly terrain on the basis of relative relief and roughness.

In reality, there is of course no sharp boundary between mountain and lowland areas as we assume it here, and the criteria for narrowing down such a boundary zone should be regarded "elastic" to some extent[18]. It has however been shown in an earlier study that the assumptions made here lead to a consistent analysis framework, and that the results are relevant in the context of water resources[2]. For the present study, we have also tested slightly altered definitions for mountain and lowland areas. These experiments did not lead to fundamentally changed patterns as compared to the ones presented here, so that our results can be considered robust.

In contrast to the upstream-downstream dichotomy that applies to all river catchments (see e.g. refs. [19,20,21]), there are basins without significant mountain areas (e.g., Dnepr River) as well as basins without significant lowland areas (e.g., the endorheic Salar de Uyuni). To obtain area-wide mapping nevertheless, a hypothetical lowland area was added to catchments that had not a single raster cell classified as lowland. This hypothetical lowland area was defined as a circular area with a radius of two raster cells, located at the lowest point of the catchment in question. In a similar fashion, a hypothetical mountain area was added at the highest point of catchments that had not a single pixel classified as mountainous. In summary analyses, however, lowland catchments with a share of mountain area of less than 5% were not assessed because the significance of runoff contributions from mountain areas might appear exaggerated. Instead, these catchments were mapped as a separate category, and their full results are found in Supplementary Fig. S10. The lowland population of catchments with a share in mountain area smaller than 5% is constantly about 11% of total lowland population (269 M in 1961–1970, 689 M in 2041–2050 under SSP2). We also tested excluding catchments with a share of mountain area of less than 10%, or not applying such a threshold at all, finding that the overall results did not change more than a few percent in most catchments. Additional context to this point is provided through an assessment of the overall contribution of mountain areas to total catchment discharge (Supplementary Fig. S11a) and setting this contribution in relation to the share that mountains have in total catchment area (Supplementary Fig. S11b). In principle, these two analyses could also have provided a threshold for excluding catchments where mountains have only minor importance in lowland hydrology. However, such a threshold already contains hydrological information. To avoid circular argumentation, we retained the strictly physiographical threshold based on area and thus on relief roughness and elevation.

Dependence of lowland areas on mountain water resources. Our assessment is based on a water balance for each raster cell of the lowland part of a catchment ($\boldsymbol{b_L}$) and an average water balance for the mountain part of the same catchment ($\overline{\boldsymbol{b}}_{\boldsymbol{M}}$) (Fig. 1a):

$$\boldsymbol{b_L}[\boldsymbol{i},\boldsymbol{j}] = \boldsymbol{r_L}[\boldsymbol{i},\boldsymbol{j}] - \boldsymbol{u_L}[\boldsymbol{i},\boldsymbol{j}] - \boldsymbol{e_L}[\boldsymbol{i},\boldsymbol{j}] \tag{1a}$$

$$\overline{\boldsymbol{b}}_{\boldsymbol{M}}[\boldsymbol{j}] = \overline{\boldsymbol{r}}_{\boldsymbol{M}}[\boldsymbol{j}] - \overline{\boldsymbol{u}}_{\boldsymbol{M}}[\boldsymbol{j}] - \overline{\boldsymbol{e}}_{\boldsymbol{M}}[\boldsymbol{j}] \tag{1b}$$

For each lowland raster cell $\boldsymbol{i}$ of catchment $\boldsymbol{j}$, $\boldsymbol{r_L}[\boldsymbol{i},\boldsymbol{j}]$ is runoff, $\boldsymbol{u_L}[\boldsymbol{i},\boldsymbol{j}]$ is consumptive water use, and $\boldsymbol{e_L}[\boldsymbol{i},\boldsymbol{j}]$ is minimum ecological flow. For the mountain area of catchment $\boldsymbol{j}$, $\overline{\boldsymbol{r}}_{\boldsymbol{M}}[\boldsymbol{j}]$ is average runoff, $\overline{\boldsymbol{u}}_{\boldsymbol{M}}[\boldsymbol{j}]$ is average consumptive water use, and $\overline{\boldsymbol{e}}_{\boldsymbol{M}}[\boldsymbol{j}]$ is average of minimum ecological flow.

We then further develop and extend the methods of ref. [2] to compute a water resources index $\boldsymbol{W}$ for each lowland raster cell $\boldsymbol{i}$ belonging to catchment $\boldsymbol{j}$ as

$$\boldsymbol{W}[\boldsymbol{i},\boldsymbol{j}] = \begin{cases} \boldsymbol{b_L}[\boldsymbol{i},\boldsymbol{j}] / \overline{\boldsymbol{b}}_{\boldsymbol{M}}[\boldsymbol{j}] & \text{if } \overline{\boldsymbol{b}}_{\boldsymbol{M}}[\boldsymbol{j}] > \boldsymbol{0} \\ \boldsymbol{0} & \text{otherwise} \end{cases} \tag{2}$$

In essence, $\boldsymbol{W}$ quantifies to what extent a raster cell in the lowlands potentially depends on mountain water surpluses. Its values are classified using the following ranges (Fig. 1b):

$\boldsymbol{W \leq -2}$: Essential, but vastly insufficient (red). The lowland raster cell has a deficit at least two times larger in absolute value than the average mountain surplus.

$\boldsymbol{-2 < W \leq -1}$: Essential, but insufficient (orange). The lowland raster cell has a deficit larger in absolute value than the average mountain surplus.

$\boldsymbol{0 < W < -1}$: Essential, and sufficient (yellow). The lowland raster cell has a deficit smaller in absolute value than the average mountain surplus.

$\boldsymbol{W = 0}$: No surplus (grey). The entire lowland basin cannot benefit from mountain surpluses.

$\boldsymbol{0 < W \leq 1}$: Supportive (green). The lowland raster cell has a surplus, but the average mountain surplus is even larger than that.

$\boldsymbol{1 \leq W < 2}$: Minor (cyan). The lowland raster cell has a surplus larger than the average mountain surplus.

$\boldsymbol{W \geq 2}$: Negligible (navy). The lowland raster cell has a surplus more than two times larger than the average mountain surplus.

Mentions of "essential" in the main text include categories "essential, and sufficient", "essential, but insufficient" and "essential, but vastly insufficient" ($\boldsymbol{W < 0}$), mentions of "essential but insufficient" encompass categories "essential, but insufficient" and "essential, but vastly insufficient" ($\boldsymbol{W \leq -1}$).

The case where mountain areas provide no surplus on average ($\boldsymbol{\bar{b}_M[j] \leq 0}$) can be due to low runoff from mountains (less than 30 mm a^{-1}, which is a threshold for permanent river flow[22]), high consumptive water use in mountain areas (more than 18.6 mm a^{-1}, which is the average value 2001–2010 for all land surface area excluding Greenland and Antarctica), or both. A distinction of these cases was not made in the main maps (Fig. 3) for reasons of clarity, but is provided separately in Supplementary Fig. S3. Note that following ref. [2], we chose a fixed threshold for high consumptive water use rather than one relative to local runoff, as such a fixed threshold is comparable across different regions world-wide. The extent of arheic mountain regions (mean decadal runoff below 3 mm a^{-1} following ref. [22]) is given for additional interpretation in Supplementary Fig. S12.

The major difference to earlier studies on "water towers"[2] is that here we can explicitly analyse lowland areas, and thus map and quantify the dependence of its population on mountain runoff. This was not feasible with the earlier typology that addressed mountain areas and compared their runoff to bulk estimates for lowland water resources. Apart from that, two further important extensions were made: First, we have implemented realistic estimates for consumptive water use, based on a global model that is calibrated against observed water consumption (see Consumptive water use, below). As compared to figures estimated from an assumed minimum per capita need and population counts (as also used in ref. [2]), this leads to lower estimates of consumptive water use in Africa, and higher estimates in Asia. In addition, it ensures that population growth does not automatically lead to increased total consumptive water use, and considers increases in water use efficiency[23] (Supplementary Fig. S8). Second, we here consider environmental minimum ecological flow, which leads to improved validity of our results for sustainable management of water resources.

In our assessment, we do not discern between lowland regions situated at different tributaries of the main river, and thus neglect possible hydrographic links to individual mountain areas within the same catchment. The only exception is the Benue River, which we separated from the Niger River and analysed as an individual catchment because its path follows a climatically very distinct route[2,24]. Here, a joint analysis would strongly confound the impact of the two rivers' mountain areas on the lowlands. After separation, the two river catchments are still of major size (Benue River: $339 \cdot 10^3$ km^2; remainder of Niger River: $1\,759 \cdot 10^3$ km^2). Further refinements in this direction should be made in future studies at the level of individual catchments.

The values of $\boldsymbol{W}$ evolve over time, reflecting changes in runoff and consumptive water use in both lowland and mountain areas (see also Drivers of changes, below).

Finally, it is important to stress that we assume mountain area surpluses, if available, to alleviate the pressure on water resources in the entire lowland part of a basin. In absence of comprehensive data, we thus refrain from implementing assumptions about water transfers that may not be correct in the individual case. Rather, we follow ref. [25] and assume that water from rivers is usually transferred effectively within a basin, and that water availability usually does not decrease much with distance from the main rivers. Where mountain surpluses are not distributed with help of engineering, they can still effect an indirect alleviation because competition for water resources from the river system is reduced in the entire lowland area of a catchment.

Water availability. To estimate water availability we used the state-of-the-art global hydrological and water resources model PCR-GLOBWB (version 2.0) that integrates human activities including water use and reservoir regulation into hydrology at a daily temporal resolution. The detailed description of the basic hydrologic model structure and associated calculation, and water use calculation, is found in ref. [26]. Below, we briefly present the main features of the model as concerns hydrologic calculations. The model's representation of consumptive water use is introduced further below.

PCR-GLOBWB simulates for each raster cell and for each time step (daily) the water storage in two vertically stacked soil layers and an underlying groundwater layer, as well as the water exchange between the layers (infiltration, percolation, and capillary rise) and between the top layer and the atmosphere (rainfall, evapotranspiration and snow melt). The model also calculates canopy interception and snow storage. Snow accumulation and melt are temperature driven and modelled according to the snow module of the Hydrologiska Byråns Vattenbalansavdelning (HBV) model[27], using fixed values for the temperature of rain-snow transition (0° C) and the degree day factor. We argue that this is sufficient for the decadal time scale we are considering, including the projections. Ice accumulation and melt are modelled via the HBV degree day method, and we do not capture the rise and subsequent decline of glacier melt runoff over the decades in a changing climate (as e.g. examined by ref. [28] while keeping constant other components of the water balance such as precipitation and evapotranspiration). Given that ice melt contributions to total runoff become small to negligible with increasing distance from the glaciers in most regions[29], this limitation of all current global models does not call into question our findings[30]. Sub-grid variability is taken into account by considering separately tall and short vegetation, paddy rice, nonpaddy crops, rainfed crop, open water (lakes, reservoirs, floodplains and wetlands), different soil types, and the area fraction of saturated soil calculated with the improved Arno scheme[31] as well as the frequency distribution of groundwater depth based on the surface elevations of the HYDRO1k Elevation Derivative Database[32]. For snow, subgrid variability is represented via elevation dependent gradients of temperature (0.65° C per 100 m) over 10 elevation zones for each raster cell, again based on HYDRO1k[30]. The groundwater store is explicitly parameterized based on lithology and topography. Natural groundwater recharge fed by net precipitation, and additional recharge fluxes from irrigation, i.e. return flow, fed by irrigation water supply and from industrial and domestic sectors occurs as the net flux from the lowest soil layer to the groundwater layer, i.e. deep percolation minus capillary rise. Groundwater recharge interacts with groundwater storage by capillary rise and baseflow.

Model outputs were processed with a robust smoothing algorithm[33] to remove artefacts. This was necessary because parts of the model input data are currently available at 30' resolution only, occasionally leading to sharp boundaries in the outputs. It was ensured that the gross water availability sum remained unchanged.

Consumptive water use. Water demands were calculated with the same model as water availability, namely PCR-GLOBWB 2. For *irrigation*, this model implements a daily scheme that separately parameterizes paddy and non-paddy crops and dynamically links with hydrological fluxes considering the feedback between the application of irrigation water and the corresponding changes in surface and soil water balance, and evapotranspiration. The losses (i.e., return flow) during water transport and irrigation application are included in the simulation based on daily evaporative and percolation losses per unit crop area based on the surface and soil water balance. For the *industrial sector*, the model calculates country-specific water use intensities based on economic development and technological improvement. *Domestic* water demand is estimated by multiplying the number of persons in a raster cell with the country-specific per capita domestic water extraction (FAO AQUASTAT; see Data availability, below). Daily water demand variations are determined using daily air temperature as a proxy[34]. The country per capita domestic water extraction in 2000 is multiplied with the estimated water use intensities to account for economic and technological development. Details are provided in ref. [34] for the past and ref. [26] for projections. For a validation of simulated sectoral water use (where data are available) see ref. [35].

As regards regionalisation of consumptive water use for the SSP scenarios, it has to be mentioned that the original IPCC SSP scenarios do not include information on specific water demands. Therefore, the present study uses state-of-the-art water demand projections based on the Water Futures and Solutions (WFaS) initiative and reported in ref. [23]. For these projections, regional sectoral water demand scenarios were constructed that are consistent with the SSP scenario storylines.

After water is withdrawn for the irrigation, industrial and domestic sectors, return flow occurs to the river system. For the irrigation sector, return flow (losses) during water transport and irrigation application are simulated based on daily evaporative and percolation losses based on the surface and soil water balance. For the industrial and domestic sectors, return flow occurs on the same day (no retention due to wastewater treatment). For the domestic sector, the return flow occurs only from the areas where urban and rural population have access to water, whereas for the industry sector, the return flow occurs from all areas where water is withdrawn. For both sectors, the amount of return flow is determined by recycling ratios developed per country. The country-specific water recycling is calculated according to the method developed in ref. [34]. For completeness, we note that consumptive water use is equal to water withdrawal minus return flow.

Model outputs were processed with the same robust smoothing algorithm that was used for water availability (see above).

Historical climate and climate scenarios. The historical forcing data set for 1961–2010 is based on time series of monthly precipitation, temperature, and reference evaporation from the CRU TS 3.2 data set[36], disaggregated to daily values with ERA40[37] (1961–1978) and ERA-Interim[38] (1979–2010) (for further details see ref. [30]). Wind-induced undercatch (particularly relevant in mountain areas) and wetting losses in precipitation have been adjusted using gridded mean monthly catch ratios[39]. For projections in the time after 2010, we used the RCP4.5 (with SSP1) and RCP6.0 (with SSP2 and SSP3) scenarios with an ensemble of 5 CMIP5 GCMs (GFDL-ESM2M, HadGEM2-ES, IPSL-CM5A-LR, MIROC-ESM-CHEM, NorESM1-M; see ref. [40]) based on the ISIMIP project (https://www.isimip.org). All analyses were done individually for each GCM first, and median and range were then computed from these results.

Downscaling. While downscaling was not necessary for the historical period, future water availability under different scenarios had to be downscaled from 30' to 5' to achieve a consistent resolution of past, present and future data. We used a delta change method in which we first aggregated our high resolution runoff values (at 5') for 2001–2010 to the lower resolution of 30'. These 30' runoff data were then compared to 30' values for 2001–2010 derived from the five GCMs we use, and grid specific differences between these two datasets were computed. These differences were then used to bias-correct the future 30' GCM data. Finally, the bias-corrected future data were compared with the aggregated 2001–2010 runoff, and differences (deltas) were derived. To achieve future runoff at 5', these deltas were multiplied with present 5' runoff. Essentially the same procedure was used for downscaling projected consumptive water use, whereas bias correction was done at country scale (rather than at grid scale as in the case of runoff) because the data required for calculating irrigation water demand are available mostly at that scale only.

Minimum ecological flow requirements. Minimum ecological flow was first computed as a fraction of total annual runoff at a resolution of 30', following the Variable Monthly Flow (VMF) method[41]. We used a uniform minimum ecological flow fraction for the whole study period to avoid introducing additional variables to our analysis. It was calculated by using average monthly runoff over 5 GCMs (GFDL-ESM2M, HadGEM2-ES, IPSL-CM5A-LR, MIROC-ESM-CHEM, NorESM1-M) in the period of 1971–2050 (ref. [40]). We could not include the 1961–1970 decade into these calculations, as data for some GCMs used start from 1971 only. This uniform fraction was then multiplied with the actual annual runoff sums to get an absolute value of minimum ecological flow for each time period analysed.

Population scenarios. Population figures at 5' resolution were extracted from the HYDE 3.2 database[42], using the SSP1, SSP2 and SSP3 pathways for projected population from 2016 onwards. We focus on the "middle of the road" pathway SSP2 and add SSP1 and SSP3 in selected results to explore the spread caused by the different pathways (Supplementary Fig. S8).

Drivers of changes. Changes in the potential dependence of lowlands on mountain water resources (water resources index $\boldsymbol{W}$, Equation 2) were analysed with a view to dominant driving factors. As a basis, we identified four potentially relevant drivers: changes in mountain runoff ($\boldsymbol{r_M}$), changes in lowland runoff ($\boldsymbol{r_L}$), changes in

mountain consumptive water use ($\boldsymbol{u_M}$), and changes in lowland consumptive water use ($\boldsymbol{u_L}$). The impact of each driver was analysed separately, keeping all other inputs constant at the level of 1961–1970. Where runoff was changed for a driver analysis, the corresponding minimum ecological flow requirements ($\boldsymbol{e_M}$, $\boldsymbol{e_L}$) were re-computed accordingly.

We then assessed the impacts of these drivers on the dependence of lowland areas on mountain water resources 2041–2050 and computed how many lowland inhabitants are changing category. As a baseline for the comparison, we assumed that runoff and total consumptive water use remain constant at the level of 1961–1970. The baseline result is thus based on the spatial patterns 1961–1970 (Fig. 3a), and applies these patterns on projected population 2041–2050.

For visualising the detailed class changes (Supplementary Fig. S13), we used the "circlize" (Circular Visualization) package for R by Zuguang Gu[43]. It follows from our methods that some changes can only be caused by certain drivers: First, a change from "supportive" (green), "minor" (cyan) or "negligible" (navy) to "essential, and sufficient" (yellow), "essential, but insufficient" (orange) or "essential, but vastly insufficient" (red) requires that the lowland water balance shifts from positive to negative. This can only be caused by changes in lowland runoff ($\boldsymbol{r_L}$), lowland consumptive water use ($\boldsymbol{u_L}$), or both. The same is true for a change in the reverse direction, where the lowland balance shifts from negative to positive. Second, any change to "no surplus" (grey) requires that the mountain water balance shifts from positive to negative, which is possible only through changes in mountain runoff ($\boldsymbol{r_M}$), mountain consumptive water use ($\boldsymbol{u_M}$), or both. This is again valid for changes in the reverse direction, where the mountain balance shifts from negative to positive.

It should be noted that we assess how many people move from one category to another, and do not consider here how big the change in $\boldsymbol{W}$ actually is. In principle, this means that small changes in $\boldsymbol{W}$ may still cause a shift in category if its value is close to a category boundary. We argue that this simplification is justifiable to obtain a clear presentation of the results, and is not a major limitation since we are mainly interested in a comparison between various scenarios.

It should further be noted that the category changes given for the individual drivers do not sum up to the overall category changes. This is because the population in a lowland raster cell may be affected by changes in more than one driver, and summing up the corresponding results is not always meaningful, e.g. when only the combined impact of more than one driver leads to a category change, or the combined impact leads to a more extensive change in category than only one driver, or when changes in opposite direction balance each other.

Hydrobelts. Hydrobelts represent an aggregation of natural hydrological basins based on similarities of their characteristic hydroclimatic features[44]. These features include annual runoff and average annual air temperature. The aggregation results in eight hydroclimatically homogeneous and near-contiguous regions, and these are used in the present study to report the regional scale results. Hydrobelts were designed specifically for high resolution analyses, and as they follow the boundaries of hydrological basins, the contrast between individual regions is more marked as compared to hydroclimatic zones, both as concerns the present state as well as the evolution over time (see ref. [44] for details). The original delineation at 30' resolution was refined to 5' with help of similarly refined coastal segments, and considers important delta areas (see Catchments, above).

Irrigated areas and food production. Spatially explicit data on areas equipped for irrigation at 5' resolution are from ref. [45]. For period 1961–1970, the average of years 1960 and 1970 was used, for period 2001–2010 the year 2005 was used. For period 2041–2050, we assumed that irrigated area is similar to period 2001–2010. Spatially explicit estimates of food production for year 2000 (5') are from ref. [46]. It should be noted that the food production data refer to both rainfed and irrigated agriculture. Interpretation of these data (Supplementary Fig. S5c, d) should therefore be made in connection with the extent of irrigated areas (Supplementary Fig. S5a, b) and bearing in mind that 40–45% of the world's food originates from irrigated agriculture[47].

Sustainability of blue water use. We used the BlWSI (blue water sustainability index) index from ref. [48] that expresses the fraction of consumptive blue water use met from non-sustainable water resources, i.e. from non-renewable groundwater abstraction and surface water over-abstraction. The index is dimensionless and ranges between 0 and 1, whereas we assumed a threshold of 0.2 to define non-sustainable use of blue water. Projected data for BlWSI are available for SSP2-RCP6.0 only, and in consequence it was not possible to examine alternative pathways.

Data availability. The following data sets were used in this study: hydrographic data from http://hydrosheds.org; elevation data from http://topotools.cr.usgs.gov/gmted_viewer and http://lta.cr.usgs.gov/hydro1k; population data from http://themasites.pbl.nl/tridion/en/themasites/hyde/download; hydroclimatic regions from http://doi.pangaea.de/10.1594/PANGAEA.806957; water extraction data from http://www.fao.org/nr/water/aquastat/main and http://geodata.grid.unep.ch; lake delineations from http://www.worldwildlife.org/pages/global-lakes-and-wetlands-database; delta area delineations from http://www.globaldeltarisk.net/data.html; food production data from http://www.earthstat.org/data-download; irrigated areas from http://mygeohub.org/publications/8.

References

1. Meybeck, M., Dürr, H. H. & Vörösmarty, C. J. Global coastal segmentation and its river catchment contributors: A new look at land-ocean linkage. *Glob. Biogeochem. Cycles* **20,** GB1S90; 10.1029/2005GB002540 (2006).
2. Viviroli, D., Dürr, H. H., Messerli, B., Meybeck, M. & Weingartner, R. Mountains of the world, water towers for humanity: Typology, mapping, and global significance. *Water Resour. Res.* **43,** W07447; 10.1029/2006WR005653 (2007).
3. Lehner, B., Verdin, K. & Jarvis, A. New global hydrography derived from spaceborne elevation data. *EOS, Trans. Am. Geophys. Union* **89,** 1–2; 10.1029/2008EO100001 (2008).
4. Lehner, B. & Grill, G. Global river hydrography and network routing. Baseline data and new approaches to study the world's large river systems. *Hydrol. Process.* **27,** 2171–2186; 10.1002/hyp.9740 (2013).
5. Gerasimov, I. P. *et al. Physio-geographical World Atlas (Atlas Mira)* (Scientific Academy of the USSR and Cartographic and Geodesic Central Committee, Moscow, 1964).
6. Tessler, Z. D. *et al.* Profiling risk and sustainability in coastal deltas of the world. *Science* **349,** 638–643; 10.1126/science.aab3574 (2015).
7. Bandyopadhyay, J., Kraemer, D., Kattelmann, R. & Kundzewicz, Z. W. in *Mountains of the World,* edited by B. Messerli & J. D. Ives (Parthenon, New York, NY, London, 1997), pp. 131–155.
8. Borsdorf, A. & Braun, V. The European and Global Dimension of Mountain Research. *Rev. Geogr. Alp.* **96,** 117–129; 10.4000/rga.630 (2008).
9. Ives, J. D., Messerli, B. & Thompson, M. Research strategy for the Himalayan region. Conference conclusions and overview. *Mt. Res. Dev.* **7,** 332–344; 10.2307/3673214 (1987).
10. Wiesmann, U. Socioeconomic Viewpoints on Highland-Lowland Systems: A Case Study on the Northwest Side of Mount Kenya. *Mt. Res. Dev.* **12,** 375; 10.2307/3673688 (1992).
11. Messerli, B. & Winiger, M. Climate, environmental change, and resources of the African Mountains from the Mediterranean to the Equator. *Mt. Res. Dev.* **12,** 315–336 (1992).
12. Weingartner, R., Viviroli, D. & Schädler, B. Water resources in mountain regions: a methodological approach to assess the water balance in a highland-lowland-system. *Hydrol. Process.* **20,** 578–585; 10.1002/hyp.6268 (2007).
13. Messerli, B. Global change and the World's mountains. Where are we coming from, and where are we going to? *Mt. Res. Dev.* **32,** S55–S63; 10.1659/MRD-JOURNAL-D-11-00118.S1 (2012).
14. Ives, J. D. in *Conservation and development in northern Thailand,* edited by J. D. Ives, Sabhasri, Sanga & P. Voraurai (United Nations University, Tokyo, 1980).
15. Meybeck, M., Green, P. A. & Vörösmarty, C. J. A new typology for mountains and other relief classes. An application to global continental water resources and population distribution. *Mt. Res. Dev.* **21,** 34–45 (2001).
16. Danielson, J. J. & Gesch, D. B. Global Multi-resolution Terrain Elevation Data 2010 (GMTED2010). USGS, 2011.
17. Fairbridge, R. W. in *The Encyclopedia of Geomorphology,* edited by R. W. Fairbridge (Rhodes, New York, NY, 1968), 745-747.
18. Browne, T., Fox, R. & Funnell, D. C. The "Invisible" Mountains. Using GIS to Examine the Extent of Mountain Terrain in South Africa. *Mt. Res. Dev.* **24,** 28–34; 10.1659/0276-4741(2004)024[0028:TIM]2.0.CO;2 (2004).
19. Green, P. A. *et al.* Freshwater ecosystem services supporting humans. Pivoting from water crisis to water solutions. *Global Environ. Chang.* **34,** 108–118; 10.1016/j.gloenvcha.2015.06.007 (2015).

20. Munia, H., Guillaume, J. H. A., Porkka, M., Wada, Y. & Kummu, M. Water stress in global transboundary river basins: significance of upstream water use on downstream stress. *Environ. Res. Lett.* **11,** 14002; 10.1088/1748-9326/11/1/014002 (2016).
21. Veldkamp, T. I. E. *et al.* Water scarcity hotspots travel downstream due to human interventions in the 20th and 21st century. *Nat. Commun.* **8,** 15697; 10.1038/ncomms15697 (2017).
22. Vörösmarty, C. J. & Meybeck, M. in *Vegetation, water, humans, and the climate,* edited by P. Kabat, *et al.* (Springer, Berlin, New York, 2004), pp. 517–572.
23. Wada, Y. *et al.* Modeling global water use for the 21st century: the Water Futures and Solutions (WFaS) initiative and its approaches. *Geosci. Model Dev.* **9,** 175–222; 10.5194/gmd-9-175-2016 (2016).
24. Viviroli, D. & Weingartner, R. The hydrological significance of mountains – from regional to global scale. *Hydrol. Earth Syst. Sci.* **8,** 1016–1029; 10.5194/hess-8-1017-2004 (2004).
25. Hanasaki, N., Yoshikawa, S., Pokhrel, Y. & Kanae, S. A global hydrological simulation to specify the sources of water used by humans. *Hydrol. Earth Syst. Sci.* **22,** 789–817; 10.5194/hess-22-789-2018 (2018).
26. Wada, Y., de Graaf, I. E. M. & van Beek, L. P. H. High-resolution modeling of human and climate impacts on global water resources. *J. Adv. Model. Earth Syst.* **8,** 735–763; 10.1002/2015MS000618 (2016).
27. Bergström, S. in *Computer models of watershed hydrology,* edited by V. P. Singh (Water Resources Publications, Highlands Ranch, Colorado (USA), 1995), pp. 443–476.
28. Huss, M. & Hock, R. Global-scale hydrological response to future glacier mass loss. *Nat. Clim. Chang.* **8,** 135–140; 10.1038/s41558-017-0049-x (2018).
29. Kaser, G., Großhauser, M. & Marzeion, B. Contribution potential of glaciers to water availability in different climate regimes. *PNAS* **107,** 20223–20227; 10.1073/pnas.1008162107 (2010).
30. Sutanudjaja, E. H. *et al.* PCR-GLOBWB 2: a 5 arcmin global hydrological and water resources model. *Geosci. Model Dev.* **11,** 2429–2453; 10.5194/gmd-11-2429-2018 (2018).
31. Hagemann, S. & Gates, L. D. Improving a subgrid runoff parameterization scheme for climate models by the use of high resolution data derived from satellite observations. *Clim. Dyn.* **21,** 349–359; 10.1007/s00382-003-0349-x (2003).
32. Verdin, K. L. & Greenlee, S. K. HYDRO1k documentation. United States Geological Survey (USGS), 1998.
33. Garcia, D. Robust smoothing of gridded data in one and higher dimensions with missing values. *Comput. Stat. Data An.* **54,** 1167–1178; 10.1016/j.csda.2009.09.020 (2010).
34. Wada, Y., Wisser, D. & Bierkens, M. F. P. Global modeling of withdrawal, allocation and consumptive use of surface water and groundwater resources. *Earth Syst. Dynam.* **5,** 15–40; 10.5194/esd-5-15-2014 (2014).
35. Wada, Y., van Beek, L. P. H. & Bierkens, M. F. P. Modelling global water stress of the recent past: on the relative importance of trends in water demand and climate variability. *Hydrol. Earth Syst. Sci.* **15,** 3785–3808; 10.5194/hess-15-3785-2011 (2011).
36. Harris, I., Jones, P. D., Osborn, T. J. & Lister, D. H. Updated high-resolution grids of monthly climatic observations – the CRU TS3.10 Dataset. *Int. J. Climatol.* **34,** 623–642; 10.1002/joc.3711 (2014).
37. Uppala, S. M. *et al.* The ERA-40 re-analysis. *Q. J. R. Meteorol. Soc.* **131,** 2961–3012; 10.1256/qj.04.176 (2005).
38. Dee, D. P. *et al.* The ERA-Interim reanalysis: Configuration and performance of the data assimilation system. *Q. J. R. Meteorol. Soc.* **137,** 553–597; 10.1002/Qj.828 (2011).
39. Adam, J. C. & Lettenmaier, D. P. Adjustment of global gridded precipitation for systematic bias. *J. Geophys. Res. Atmos.* **108,** 4257; 10.1029/2002JD002499 (2003).
40. Hempel, S., Frieler, K., Warszawski, L., Schewe, J. & Piontek, F. A trend-preserving bias correction – the ISI-MIP approach. *Earth Syst. Dynam.* **4,** 219–236; 10.5194/esd-4-219-2013 (2013).
41. Pastor, A. V., Ludwig, F., Biemans, H., Hoff, H. & Kabat, P. Accounting for environmental flow requirements in global water assessments. *Hydrol. Earth Syst. Sci.* **18,** 5041–5059; 10.5194/hess-18-5041-2014 (2014).
42. Klein Goldewijk, K., Beusen, A., Doelman, J. & Stehfest, E. Anthropogenic land use estimates for the Holocene – HYDE 3.2. *Earth Syst. Sci. Data* **9,** 927–953; 10.5194/essd-9-927-2017 (2017).
43. Gu, Z., Gu, L., Eils, R., Schlesner, M. & Brors, B. circlize implements and enhances circular visualization in R. *Bioinformatics* **30,** 2811–2812; 10.1093/bioinformatics/btu393 (2014).
44. Meybeck, M., Kummu, M. & Dürr, H. H. Global hydrobelts and hydroregions: improved reporting scale for water-related issues? *Hydrol. Earth Syst. Sci.* **17,** 1093–1111; 10.5194/hess-17-1093-2013 (2013).

45. Siebert, S. *et al.* A global data set of the extent of irrigated land from 1900 to 2005. *Hydrol. Earth Syst. Sci.* **19,** 1521–1545; 10.5194/hess-19-1521-2015 (2015).
46. Mueller, N. D. *et al.* Closing yield gaps through nutrient and water management. *Nature* **490,** 254–257; 10.1038/nature11420 (2012).
47. Döll, P. & Siebert, S. Global modeling of irrigation water requirements. *Water Resour. Res.* **38,** 1037; 10.1029/2001WR000355 (2002).
48. Wada, Y. & Bierkens, M. F. P. Sustainability of global water use. Past reconstruction and future projections. *Environ. Res. Lett.* **9,** 104003; 10.1088/1748-9326/9/10/104003 (2014).
49. Körner, C. *et al.* A global inventory of mountains for bio-geographical applications. *Alp Botany* **127,** 1–15; 10.1007/s00035-016-0182-6 (2017).

Supplementary material for:
Increasing dependence of lowland population on mountain water resources

Daniel Viviroli[1,*], Matti Kummu[2], Michel Meybeck[3], Yoshihide Wada[4,5]

[1] Department of Geography, University of Zürich, Switzerland
[2] Water & Development Research Group, Aalto University, Espoo, Finland
[3] Université Pierre et Marie Curie, Paris, France
[4] International Institute for Applied Systems Analysis, Laxenburg, Austria
[5] Department of Physical Geography, Faculty of Geosciences, Utrecht University, The Netherlands

*** Corresponding author:**
Daniel Viviroli (daniel.viviroli@geo.uzh.ch)
Hydrology and Climate, Department of Geography, University of Zürich
Winterthurerstr. 190, CH-8057 Zürich, Switzerland

This is a non-peer reviewed preprint submitted to EarthArXiv

Supplementary Text

Results from projections with alternative scenarios

To test the sensitivity of our projected results towards scenarios, we ran the analysis for the SSP1-RCP4.5, SSP2-RCP6.0 and SSP3-RCP6.0 pathways. In terms of global-scale patterns, results show no major differences, and the share of people residing in the individual classes in 2041–2050 does not differ by more than 1–2% between scenarios (Supplementary Fig. S14). The share of total lowland population depending on essential contributions from mountain areas ranges between 38.5% (SSP1-RCP4.5) and 40.1% (SSP3-RCP6.0). However, the absolute number of people assigned to the classes differs more strongly between scenarios because the growth in total population diverges in the underlying SSPs (Supplementary Fig. S8): The absolute lowland population projected to depend on essential contributions from mountain areas ranges between 2.3 B (SSP1-RCP4.5) and 2.7 B (SSP3-RCP6.0). At the level of hydrobelts, the largest differences in dependency on mountain areas are found where population development also shows wider divergence between scenarios, such as in the North suptropical hydrobelt. Scenario differences between projected per-capita consumptive water use, on the other hand, seem less important, as can be seen in the Boreal hydrobelt. The individual GCM members of the scenarios examined show high agreement in wide parts of the lowland area (Supplementary Fig. S15). Examples for a widespread lower agreement are found in parts of the Amazon River basin and on the Arabian Peninsula, where lowland population density is generally low.

Simulated water availability in mountain areas

A known issue of current macroscale hydrological models is that they tend to underestimate mean annual discharge over mountainous areas[1]. For PCR-GLOBWB 2, however, it has been shown that model efficiency at daily time step has improved significantly for areas above 1 000 m a.s.l. with using 5' instead of 30' resolution (as in this study), and is only slightly inferior to efficiency below 1 000 m a.s.l. (Supplementary Fig. S16). The comparison was done at ~3 600 Global Runoff Data Center (GRDC) sites and highlights the advantages of using 5' resolution for assessing the dependency of lowlands on mountain runoff (see ref. [2] for details).

We further compared PCR-GLOBWB 2 mean annual discharge 1961–2010 to long-term mean annual discharge reported in the Global Streamflow Characteristics Dataset (GSCD)[1]. GSCD has no explicit timeframe due to the use of records with a broad range of start dates and duration, and it should be mentioned that the dataset is similarly limited by the general lack of hydrometeorological observations at high elevations[3] as any global hydrological model is. An analysis for 100 m elevation bands (Supplementary Fig. S17) shows that

PCR-GLOBWB 2 and GSCD results agree to a high degree at global scale, with PCR-GLOBWB 2 generally having slightly lower discharge values. Similarly high agreement is found in the North mid-latitude, North subtropical, Equator, South subtropical and South dry hydrobelts. The first two of these are the most populous of all global hydrobelts, with 3.10 B and 1.42 B lowland inhabitants in the 2000s, respectively, and encompassing over 70% of total lowland population. Increasing disagreement towards low elevations is apparent in the Boreal and South mid-latitude hydrobelts, where PCR-GLOBWB 2 shows lower values than GSCD. Lowland population counts are only 0.10 and 0.09 B, respectively. Some disagreement at high elevations is noted in the North dry hydrobelt (0.63 B lowland inhabitants), where GSCD generally shows a smoother decline of discharge with elevation than PCR-GLOBWB 2. Between roughly 2 000–4 000 m a.s.l., GSCD discharge is higher, above that PCR-GLOBWB 2 discharge.

Finally, we tested the robustness of our analysis framework by adjusting PCR-GLOBWB 2 runoff to GSCD runoff. In detail, we computed a cell-by-cell adjustment factor from PCR-GLOBWB 2 (1961–2010) to GSCD (no explicit timeframe), limited the adjustment factor to a range of 0.2–5.0 to avoid highly implausible results in areas with low runoff and then applied it to PCR-GLOBWB 2 mean annual runoff 2001–2010. Simulated consumptive water use was left unchanged. It has to be mentioned that GSCD should actually not be used for catchments larger than 10 000 km². This limitation in scale seems less important for our cell-by-cell assessment of lowland regions but could still be relevant in the average water balance we set up for the mountain parts of larger river basins.

The comparison of results for 2001–2010 reveals that adjusted PCR-GLOBWB 2 data assigns more people to the "essential but sufficient" category (28% instead of 21%) and less to the "minor" category (6% instead of 11%) (Supplementary Fig. S18). Differences in the other categories are small. It should be stressed again that also the GSCD data are subject to considerable uncertainty at higher elevations (especially in South America, Africa and Asia) due to the scarcity of direct observations of runoff. Because of these limitations and because GSCD has an ambiguous timeframe, we kept using the unadjusted PCR-GLOBWB 2 that implies a slightly lower dependence of lowland inhabitants on mountain water resources.

An assessment based on additional global hydrological and water resources models would be desirable in the future to further quantify uncertainties, but was not feasible for this study as such data are currently not available from other models at the resolution we are using.

To conclude, it has to be stressed that our goal is a global overview. We identify lowland regions that show critical dependence on mountain water resources, and recognise past trends and possible future developments relevant for water resources management in the context of highland-lowland interactions. Such analyses depend on Global Hydrological Models (GHMs), and these are in turn limited in terms of accuracy, depiction of physical processes and parameterisation of human impacts, especially in upstream catchments[4]. Within the scope of our analysis, i.e. for studying decadal patterns and related changes at global scale, GHMs can be considered highly useful and adequate tools. When it comes to specific river basins and details of water resources management at seasonal scale, however, regional hydrological models should be employed[5].

Development of consumptive water use

Figures for simulated per-capita consumptive water use 1961–2050 are shown in Supplementary Fig. S8, revealing a relatively stable global average around 400 $m^3\ p^{-1}\ a^{-1}$ for the lowlands and slightly lower values for mountain areas, where a decrease from 385 (1961–1970) to 330 $m^3\ p^{-1}\ a^{-1}$ (2041–2050, median of the three SSP-RCP scenarios) is noted. At the level of hydrobelts, increasing per-capita values in both mountain and lowland areas are found in the Boreal (mainly driven by Eastern Europe) and the North mid-latitude hydrobelts, as well as in the South mid-latitude belt (mainly driven by Australia, in the lowlands however with a decline after 2001–2010). Decreasing values are found in the North dry, North subtropical, Equator and South dry hydrobelts.

Drivers of changes

In the results for the "no surplus" (grey) category, the impacts of the individual drivers reported in Table 2 (+3 M lowland people for changed mountain runoff; +171 M for changed mountain consumptive water use) fall strikingly short of the overall impact (+316 M). This is because the entire lowland of a catchment is either fully in the "no surplus" category or not at all (see Methods), and some catchments move into this category only through the combined impact of changes in mountain runoff and consumptive water use. The most important

cases in this respect are found on the Indian Peninsula, namely the Krishna (lowland population of 83 M in 2041–2050), Sabarmati (21 M) and Penneru (10 M) River catchments (Supplementary Table S1).

Supplementary Methods

Disproportionality of mountain runoff. We examine the relation of mountain runoff to average lowland runoff by computing, for each mountain raster cell, a disproportionality factor $\boldsymbol{D}$ as

$$\boldsymbol{D}[\boldsymbol{i},\boldsymbol{j}] = \frac{\boldsymbol{r_M}[\boldsymbol{i},\boldsymbol{j}]}{\bar{\boldsymbol{r}}_{\boldsymbol{L}}[\boldsymbol{j}]} \quad \text{(S1)}$$

where $\boldsymbol{r_M}[\boldsymbol{i},\boldsymbol{j}]$ is the runoff of mountain cell $\boldsymbol{i}$ belonging to basin $\boldsymbol{j}$ and $\bar{\boldsymbol{r}}_{\boldsymbol{L}}[\boldsymbol{j}]$ is average lowland runoff in basin $\boldsymbol{j}$. This computation is used as a basis for Supplementary Figs. S6 and S7.

References

1. Beck, H. E., de Roo, A. & van Dijk. Global Maps of Streamflow Characteristics Based on Observations from Several Thousand Catchments. *J. Hydrometeorl.* **16,** 1478–1501; 10.1175/JHM-D-14-0155.1 (2015).
2. Sutanudjaja, E. H. *et al.* PCR-GLOBWB 2: a 5 arcmin global hydrological and water resources model. *Geosci. Model Dev.* **11,** 2429–2453; 10.5194/gmd-11-2429-2018 (2018).
3. Viviroli, D. *et al.* Climate change and mountain water resources: overview and recommendations for research, management and policy. *Hydrol. Earth Syst. Sci.* **15,** 471–504; 10.5194/hess-15-471-2011 (2011).
4. Veldkamp, T. I. E. *et al.* Human impact parameterizations in global hydrological models improves estimates of monthly discharges and hydrological extremes: a multi-model validation study // Human impact parameterizations in global hydrological models improve estimates of monthly discharges and hydrological extremes: a multi-model validation study. *Environ. Res. Lett.* **13,** 55008; 10.1088/1748-9326/aab96f (2018).
5. Hattermann, F. F. *et al.* Cross ‐ scale intercomparison of climate change impacts simulated by regional and global hydrological models in eleven large river basins. *Climatic Change* **141,** 561–576; 10.1007/s10584-016-1829-4 (2017).
6. Körner, C. *et al.* A global inventory of mountains for bio-geographical applications. *Alp Botany* **127,** 1–15; 10.1007/s00035-016-0182-6 (2017).
7. Meybeck, M., Kummu, M. & Dürr, H. H. Global hydrobelts and hydroregions: improved reporting scale for water-related issues? *Hydrol. Earth Syst. Sci.* **17,** 1093–1111; 10.5194/hess-17-1093-2013 (2013).
8. Misra, A. K. *et al.* Proposed river-linking project of India. A boon or bane to nature. *Environ. Geol.* **51,** 1361–1376; 10.1007/s00254-006-0434-7 (2007).
9. Ghassemi, F. & White, I. *Inter-Basin Water Transfer. Case studies from Australia, United States, Canada, China, and India* (Cambridge University Press, New York, NY, 2007).
10. Gupta, H. V., Kling, H., Yilmaz, K. K. & Martínez, G. F. Decomposition of the mean squared error and NSE performance criteria: Implications for improving hydrological modelling. *J. Hydrol.* **377,** 80–91; 10.1016/j.jhydrol.2009.08.003 (2009).

Supplementary Tables

Supplementary Table S1. Lowland population 1961–2050 in areas with no surplus from mountains 2041–2050. Details are shown for all river catchments with a lowland population of 10 M or more that do not receive contributions from mountain areas in 2041–2050. The numbers are given in Million people. Results refer to catchments with a share of mountain area in total area of at least 5%, and to the SSP2-RCP6.0 scenario for projections. See also Supplementary Table S2.

#	*River catchment*	*1961–1970*	*2001–2010*	*2041–2050*[a]	*Major mountain range(s), hills and plateau(x)*[b]	*Share of mountain area in total area*	*Hydrobelt*[c]
1	Krishna[d]	0.0	0.0	83.2^{+++}	Western Ghats, Eastern Ghats	31%	NST
2	Hai He[e]	43.7	81.6	81.0^{+++++}	Taihang Mountains, Yin Mountains, Mount Wutai, Mount Heng	56%	NML
3	Huang He (Yellow)[e]	0.0	0.0	59.0^{+++++}	Tibetan Plateau, Lüliang Mountains, Kunlun Mountains	88%	NML
4	Liao	0.0	0.0	23.9^{+++++}	Changbai Mountains	43%	NML
5	Sabarmati[f]	0.0	0.0	21.0^{+++++}	Aravalli Range	16%	NST
6	Penneru[d]	0.0	7.0	10.1^{+++++}	Eastern Ghats, Nandi Hills	47%	NST
	Remaining catchments	*26.8*	*134.2*	*173.0*			
	Total	***70.5***	***222.8***	***451.2***			

[a] SSP2-RCP6.0 pathway. The computation of bounds is not sensible here because either the entire lowland population is affected by the lack of surplus from mountains, or none of it (Methods). Instead, the number of pluses ($^{+}$) behind the values indicates how many of the five ensemble members see the lowland population affected by a lack of surplus from mountains in 2041–2050.

[b] following ref. [6] and area labels of major physiographic features provided by Natural Earth (version 3.0.0, available at http://www.naturalearthdata.com)

[c] NML: North mid-latitude; NST: North subtropical (see ref. [7])

[d] Part of the proposed river-linking project in India (peninsular part)[8]

[e] Part of the South-to-North Water Transfer Project in China[9]

[f] Part of the proposed river-linking project in India (Himalayan part)[8]

Supplementary Table S2. Lowland population depending on essential mountain runoff contributions 1961–2050, further catchments. Details are shown for river catchments mentioned in the main text but not appearing in Table 1 because the lowland population depending on essential mountain runoff contributions 2041–2050 is smaller than 10 Million. Details are also given for the catchments appearing in Supplementary Table S1. The numbers are in Million people and encompass all areas depending on mountain contributions that are essential and sufficient (yellow), essential but insufficient (orange) and essential but vastly insufficient (red). Results refer to catchments with a share of mountain area in total area of at least 5%, and to the SSP2-RCP6.0 scenario for projections.

#	*River catchment*	*1961–1970*	*2001–2010*	*2041–2050*[a]	*Major mountain range(s), hills and plateau(x)*[b]	*Share of mountain area in total area*	*Hydrobelt*[c]
28	Grande [US and Mexico][d]	2.0	5.4	$7.4^{+0.0}_{-0.4}$	Mexican Plateau, Sierra Madre Occidental, Sierra Madre Oriental, Rocky Mountains	85%	NDR
37	Colorado [US and Mexico]	1.1	3.8	$5.1^{+0.0}_{-0.0}$	Rocky Mountains, Colorado Plateau	94%	NDR
-	Huang He (Yellow)[e]	30.2	58.9	$0.0^{+0.0}_{-0.0}$	Tibetan Plateau, Lüliang Mountains, Kunlun Mountains	88%	NML
-	Krishna[e]	5.6	52.2	$0.0^{+0.0}_{-0.0}$	Western Ghats, Eastern Ghats	31%	NST
-	Liao[e]	10.2	23.3	$0.0^{+0.0}_{-0.0}$	Changbai Mountains	43%	NML
-	Sabarmati[e]	1.1	13.4	$0.0^{+0.0}_{-0.0}$	Aravalli Range	16%	NST
-	Penneru[f]	1.1	0.0	$0.0^{+0.0}_{-0.0}$	Eastern Ghats, Nandi Hills	47%	NST
-	Hai He[g]	0.0	0.0	$0.0^{+0.0}_{-0.0}$	Taihang Mountains, Yin Mountains, Mount Wutai, Mount Heng	56%	NML

[a] ensemble median for SSP2-RCP6.0, with differences to the ensemble minimum and maximum added in subscript and superscript, respectively

[b] following ref. [6] and area labels of major physiographic features provided by Natural Earth (version 3.0.0, available at http://www.naturalearthdata.com)

[c] NML: North mid-latitude; NDR: North dry; NST: North subtropical (see ref. [7])

[d] For of the Rio Grande, one GCM ensemble member sees the entire lowland population receiving no more surplus from mountain areas in 2041–2050. This ensemble member was not used for computing the bounds shown here.

[e] For these rivers, there is no surplus from mountain areas 2041–2050. Surpluses cease 2011–2020 for the Sabarmati, 2021–2030 for the Liao and the Yellow, and 2041–2050 for the Krishna River (Supplementary Table S1, Supplementary Fig. S4).

[f] For the Penneru River, there is no surplus from mountain areas from 1981–1990 onwards (Supplementary Table S1, Supplementary Fig. S4).

[g] For the Hai He River, there is no surplus from mountain areas from 1961–1970 onwards (Supplementary Table S1, Supplementary Fig. S4).

Supplementary Table S3. Countries depending on essential mountain runoff contributions 1961–2050. Details are shown for all countries with a lowland population of 10 M or more in 2041–2050 that potentially depend on essential mountain runoff contributions. The numbers are given in Million people. Note that Bangladesh, although having a share of mountain area in total country area of only 2%, receives extensive contributions from mountains originating upstream of the country in the Ganges-Brahmaputra-Meghna River basin. Similar, albeit less extreme examples are Iraq, Sudan and the Syrian Arab Republic. Results refer to the SSP2-RCP6.0 scenario for projections.

Country	*1961–1970*	*2001–2010*	*2041–2050*[a]	*Share of mountain area in total country area*
India	153.8	604.1	$799.6^{+63.1}_{-6.3}$	28%
China	217.0	431.1	$460.8^{+41.2}_{-10.6}$	74%
Pakistan	40.8	107.4	$193.1^{+3.6}_{-1.2}$	51%
Egypt	31.5	72.9	$117.6^{+0.0}_{-0.0}$	13%
Russian Federation	29.9	68.9	$82.9^{+1.4}_{-1.2}$	37%
Indonesia	9.0	46.8	$76.1^{+10.9}_{-1.3}$	38%
Nigeria	1.2	20.5	$61.4^{+4.7}_{-17.7}$	13%
United States of America	7.6	29.2	$55.1^{+3.1}_{-7.6}$	46%
Iraq	7.2	24.1	$54.4^{+2.1}_{-5.0}$	9%
Viet Nam	0.0	25.0	$43.6^{+12.2}_{-1.4}$	53%
Japan	20.0	29.1	$41.7^{+4.4}_{-1.6}$	59%
Niger	0.7	9.4	$39.5^{+1.6}_{-6.8}$	9%
Sudan	3.8	20.3	$34.4^{+2.2}_{-0.3}$	13%
Bangladesh	0.0	23.9	$30.1^{+5.5}_{-11.0}$	2%
Thailand	7.1	21.1	$26.3^{+3.9}_{-1.2}$	36%
Korea, Republic of	0.0	17.2	$24.4^{+0.6}_{-0.9}$	46%
Uzbekistan	7.2	18.5	$23.5^{+0.0}_{-0.0}$	16%
Philippines	0.0	13.1	$20.9^{+2.2}_{-2.4}$	43%
Ukraine	6.5	15.4	$18.3^{+1.2}_{-0.1}$	5%
Nepal	0.0	10.3	$18.1^{+1.2}_{-0.8}$	86%
Canada	2.0	3.7	$17.6^{+0.4}_{-1.0}$	31%
France	4.8	12.2	$16.3^{+0.8}_{-0.4}$	30%
Argentina	2.0	4.4	$16.1^{+3.4}_{-1.0}$	34%
Poland	0.1	5.0	$15.1^{+1.1}_{-1.4}$	7%
Morocco	3.6	9.4	$13.7^{+0.8}_{-0.2}$	43%
Mexico	2.8	9.0	$13.7^{+0.1}_{-5.5}$	71%
Syrian Arab Republic	1.3	8.9	$12.4^{+0.1}_{-0.9}$	27%
Ghana	0.0	1.0	$12.3^{+4.0}_{-9.2}$	4%
Kazakhstan	4.7	7.5	$10.6^{+0.0}_{-0.3}$	15%
Iran	2.7	8.2	$10.2^{+0.7}_{-0.6}$	82%

[a] ensemble median for SSP2-RCP6.0, with differences to the ensemble minimum and maximum added in subscript and superscript, respectively

Supplementary Table S4. Lowland population benefiting from supportive mountain runoff contributions 1961–2050. Details are shown for all river catchments with a lowland population of 10 M or more in 2041–2050 that benefit from supportive mountain contributions. The numbers are given in Million people. Results refer to catchments with a share of mountain area in total area of at least 5%, and to the SSP2-RCP6.0 scenario for projections.

#	*River catchment*	*1961–1970*	*2001–2010*	*2041–2050*[a]	*Major mountain range(s), hills and plateau(x)*[b]	*Share of mountain area in total area*	*Hydrobelt*[c]
1	Ganges-Brahmaputra-Meghna	109.3	132.5	$224.1^{+8.3}_{-16.4}$	Himalayas, Mishmi Hills, Meghalaya Hills	44%	NML
2	Rhine-Meuse-Scheldt	44.2	52.3	$51.2^{+0.6}_{-0.7}$	European Alps, Black Forest, Jura Mountains, Vosges	44%	NML
3	Niger[d]	15.4	27.8	$50.8^{+16.9}_{-6.5}$	Guinea Highlands, Fouta Djallon, Aïr massif	8%	NST
4	Chang Jiang (Yangtze)	61.1	79.7	$46.3^{+3.7}_{-11.8}$	Yunnan-Guizhou Plateau, Tibetan Plateau, Bayan Har Mountains, Shaluli Mountains	69%	NML
5	St. Lawrence	28.6	41.5	$45.1^{+1.2}_{-1.0}$	Superior Upland, Adirondack Mountains, Laurentian Mountains, Appalachian Mountains	9%	NML
6	Nile	8.1	14.9	$34.6^{+0.4}_{-1.9}$	Ethiopian Highlands[d], Albertine Rift Mountains[e], Nuba Mountains	33%	NDR
7	Benue[d]	5.0	13.2	$31.3^{+1.4}_{-0.1}$	Adamawa Plateau, Jos Plateau	37%	NST
8	Parana	9.3	18.4	$26.5^{+1.3}_{-2.9}$	Cordillera Oriental [Argentina, Bolivia], Mantiqueira Mountains	32%	SST
9	Mahanadi	10.8	16.5	$25.7^{+3.3}_{-3.1}$	Eastern Ghats, Chota Nagpur Plateau, Satpura Range	31%	NST
10	Cross	3.9	10.6	$25.3^{+0.8}_{-0.9}$	Adamawa Plateau	22%	EQT
11	Danube	36.4	34.6	$23.0^{+1.1}_{-1.2}$	Carpathian Mountains, European Alps, Dinaric Alps, Balkan Mountains	52%	NML
12	Mekong	10.2	23.1	$22.1^{+3.6}_{-2.9}$	Annamese Cordillera, Luang Prabang Range, Shan Plateau, Tanggula Mountains	54%	NST
13	Zhujiang (Pearl)-Xi Jiang (West)-Bei Jiang (North)-Dong Jiang (East)	8.7	32.1	$20.4^{+3.7}_{-9.7}$	Yunnan-Guizhou Plateau, Nanling Mountains	73%	NST
14	Congo	3.9	5.6	$19.3^{+5.9}_{-5.3}$	Katanga Plateau, Albertine Rift Mountains	51%	EQT
15	Damodar	5.6	10.4	$16.6^{+4.6}_{-3.5}$	Chota Nagpur Plateau	13%	NML
16	Brahmani	4.6	8.6	$13.6^{+0.7}_{-5.0}$	Chota Nagpur Plateau, Eastern Ghats	45%	NST
17	Po	11.1	12.7	$12.6^{+0.5}_{-0.3}$	European Alps, Apennine Range	63%	NML

[Table continued on next page]

18	Irrawaddy	4.2	14.2	$11.1^{+0.6}_{-0.5}$	Hengduan Mountains, Chin Hills, Shan Hills, Patkai Range	59%	NST
19	Amazon	1.2	5.6	$10.9^{+1.3}_{-3.2}$	Cordillera Oriental [Peru, Bolivia], Cordillera Occidental [Peru, Bolivia, Chile], Cordillera Central [Ecuador]	15%	EQT
20	Godavari	18.4	12.4	$10.7^{+3.4}_{-2.0}$	Eastern Ghats, Western Ghats	22%	NST
21	Elbe	16.0	12.9	$10.0^{+0.5}_{-1.8}$	Ore Mountains, Bohemian Forest, Sudeten, Harz	33%	NML
	Remaining catchments	*641.9*	*918.0*	$1\,029.2^{+76.6}_{-75.1}$			
	Total	***1,058.2***	***1,497.5***	$\mathbf{1\,760.1^{+140.2}_{-156.1}}$			

[a] ensemble median for SSP2-RCP6.0, with differences to the ensemble minimum and maximum added in subscript and superscript, respectively

[b] following ref. [6] and area labels of major physiographic features provided by Natural Earth (version 3.0.0, available at http://www.naturalearthdata.com)

[c] BOR: boreal; NML: North mid-latitude; NDR: North dry; NST: North subtropical; EQT: Equatorial; SST: South subtropical

[d] The Benue River was separated from the Niger River because the paths of these two rivers follow climatically very different routes (Methods).

[e] for the Blue Nile River

[f] for the White Nile River

[g] The entire lowland part of the Yellow River catchment receives no more surplus from mountains from 2021–2030 onwards (Supplementary Table S1, Supplementary Fig. S4).

Supplementary Table S5. Food production characteristics in 2000 by hydrobelt. Results are for caloric values and further differentiated into contributions of mountain and lowland areas to total global food production.

Hydrobelt	*Food production [10^{15} kcal a^{-1}]*	*Contribution to global food production*	
		Mountain area	*Lowland area*
Boreal	0.63	0.4%	3.3%
North mid-latitude	8.18	8.1%	39.9%
North dry	0.84	2.4%	2.6%
North subtropical	2.96	5.1%	12.3%
Equatorial	1.70	3.7%	6.3%
South subtropical	2.16	5.5%	7.2%
South dry	0.11	0.3%	0.3%
South mid-latitude	0.46	0.7%	2.0%
All hydrobelts	**17.03**	**26.2%**	**73.8%**

Supplementary Table S6. Area equipped for irrigation in 2005 by hydrobelt. Results are further differentiated into mountain and lowland areas.

Hydrobelt	*Area equipped for irrigation [10^3 km^2]*	*Share in global area equipped for irrigation*	
		Mountain area	*Lowland area*
Boreal	65	0.4%	1.8%
North mid-latitude	1 676	11.1%	43.7%
North dry	524	7.2%	9.9%
North subtropical	471	3.4%	12.0%
Equatorial	144	1.4%	3.3%
South subtropical	73	1.1%	1.3%
South dry	21	0.5%	0.2%
South mid-latitude	82	0.7%	1.9%
All hydrobelts	**3 056**	**25.8%**	**74.2%**

Supplementary Figures

Supplementary Figure S1. Relief roughness and elevation classes used for distinguishing mountain and lowland areas. The map shows the global mountain (a) and lowland (b) areas as defined in the Methods section (see main text), both excluding Greenland and Antarctica. Large lakes (>50 km^2) are drawn here using their actual relief roughness (which is zero) rather than the assumed average roughness used for distinguishing mountain and lowland areas (Methods). The boundaries of catchments with an area of 100 000 km² and more are drawn for orientation.

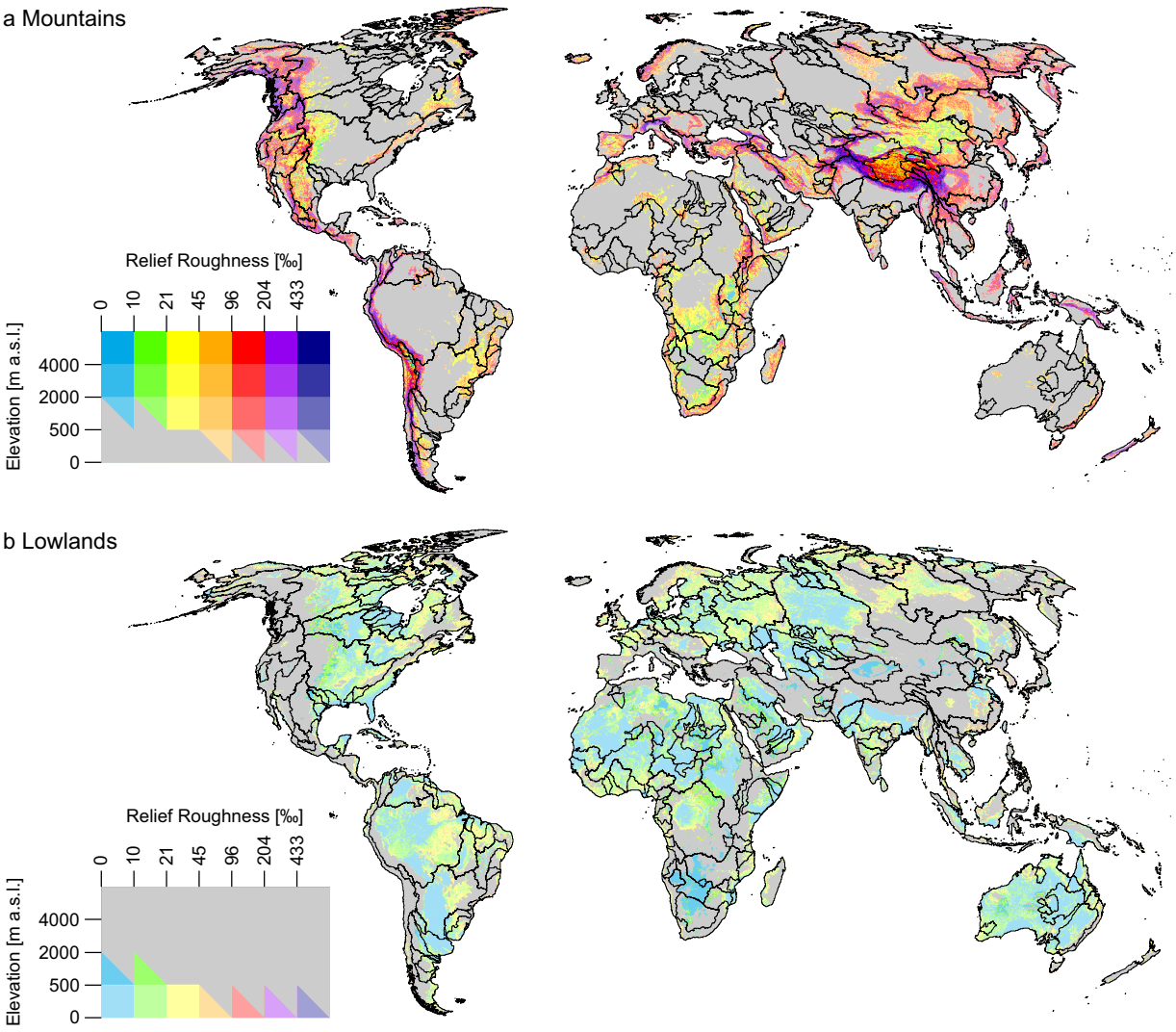

Supplementary Figure S2. Share of lowland population depending on mountain water resources 1961–2050. Results are shown as fractions of the respective population totals (decadal averages), summarised for all hydrobelts (a) as well as differentiated by hydrobelt (b–i). For absolute values see Fig. 2 in main article.

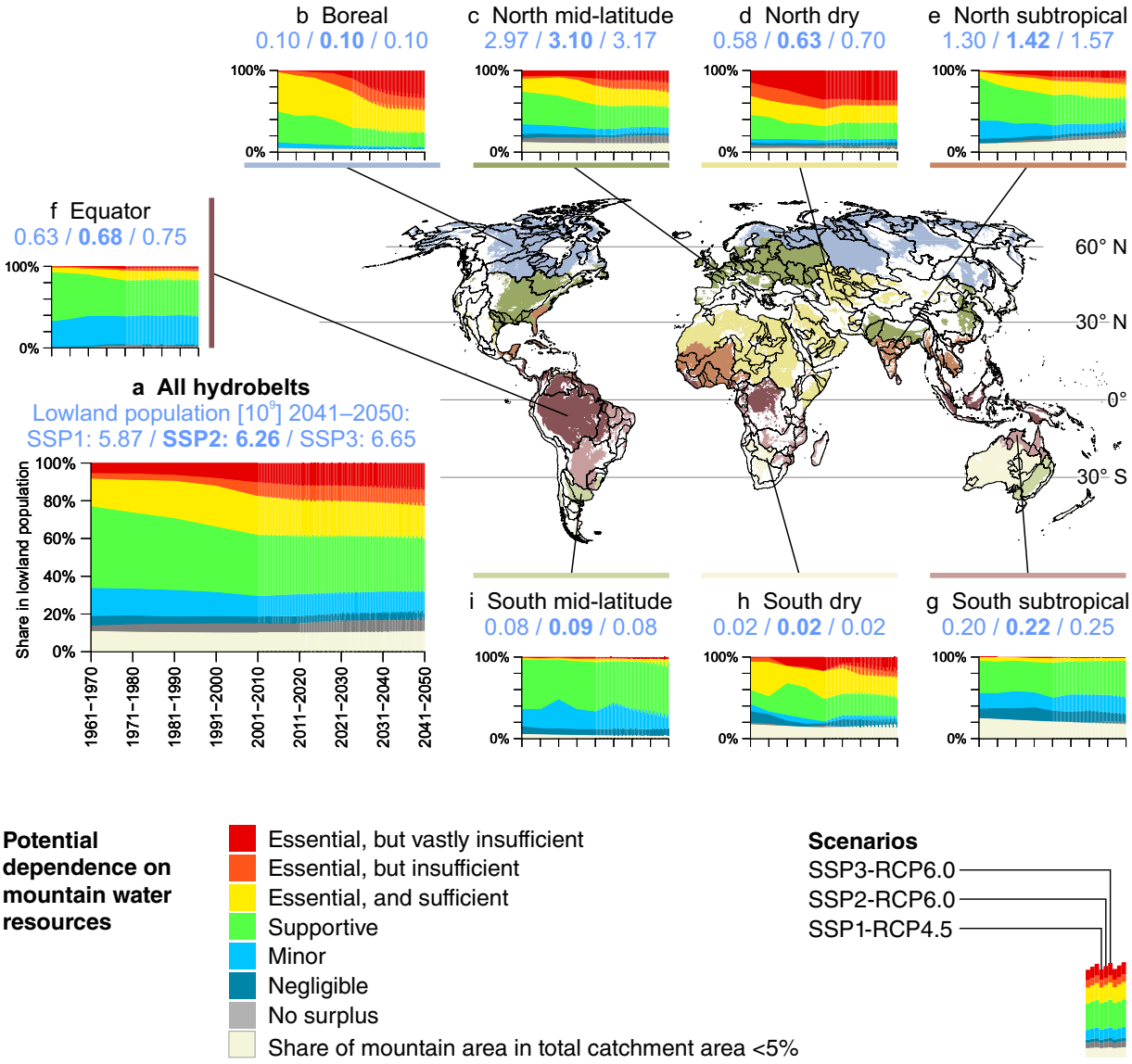

Supplementary Figure S3. Causes of missing surplus from mountain areas as well as water balance of lowlands receiving no surplus from mountain areas 1961–2050. Global results are shown for the time periods 1961–1970 (a, b), 2001–2010 (c, d) and 2041–2050 (e, f), magnifications for selected regions for 2041–2050 only (g–j and k–n). The boundaries of catchments with an area of 100 000 km² and more are drawn for orientation, and projections refer to the SSP2-RCP6.0 scenario.

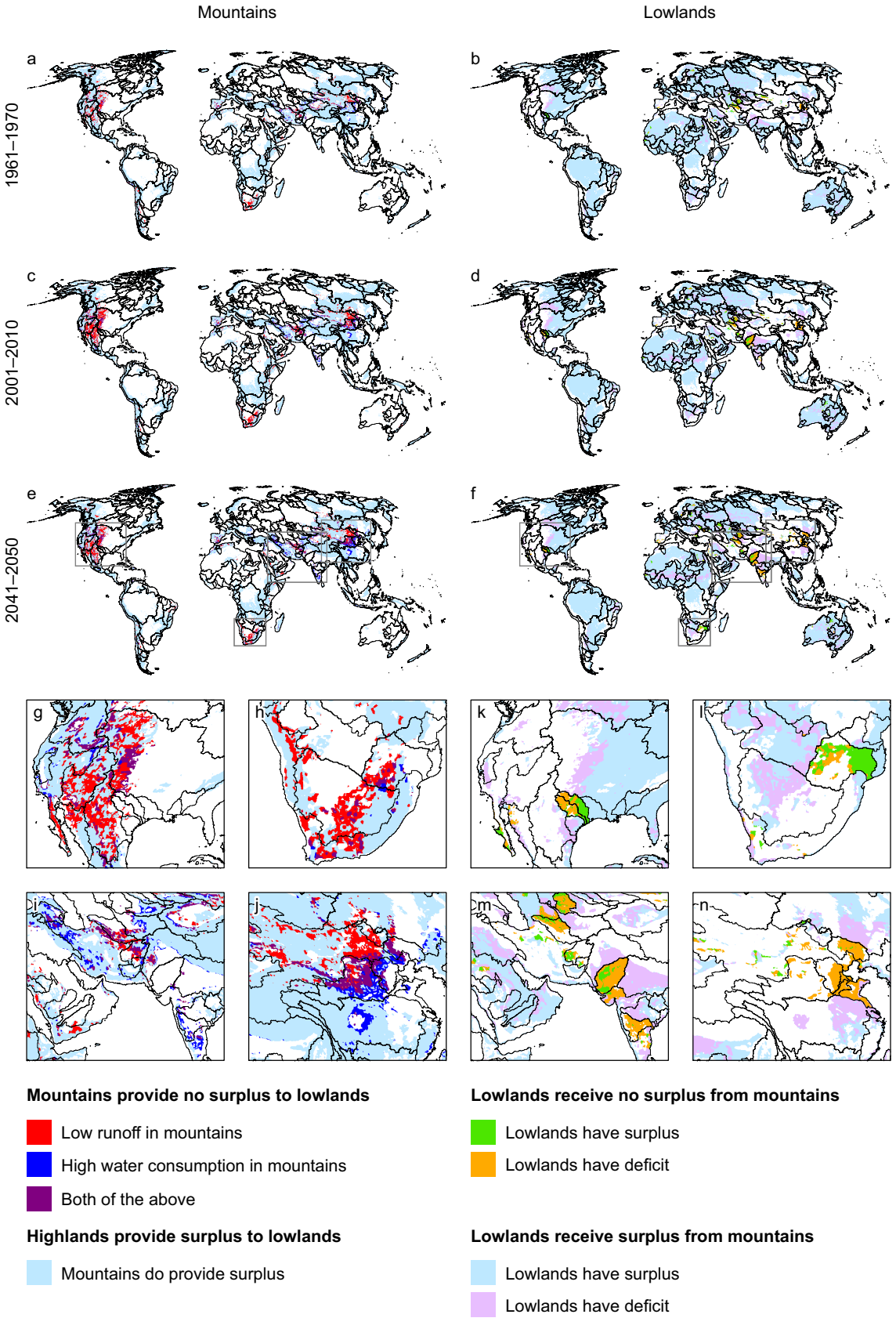

Supplementary Figure S4. First occurrence of missing surplus from mountain areas. The map shows for which lowland areas a lack of mountain runoff surplus occurs in 2041–2050, and indicates the decade in which an uninterrupted lack has started. In addition, the map differentiates whether there is a water balance deficit in the lowland area 2041–2050. The boundaries of catchments with an area of 100 000 km² and more are drawn for orientation, and projections refer to the SSP2-RCP6.0 scenario.

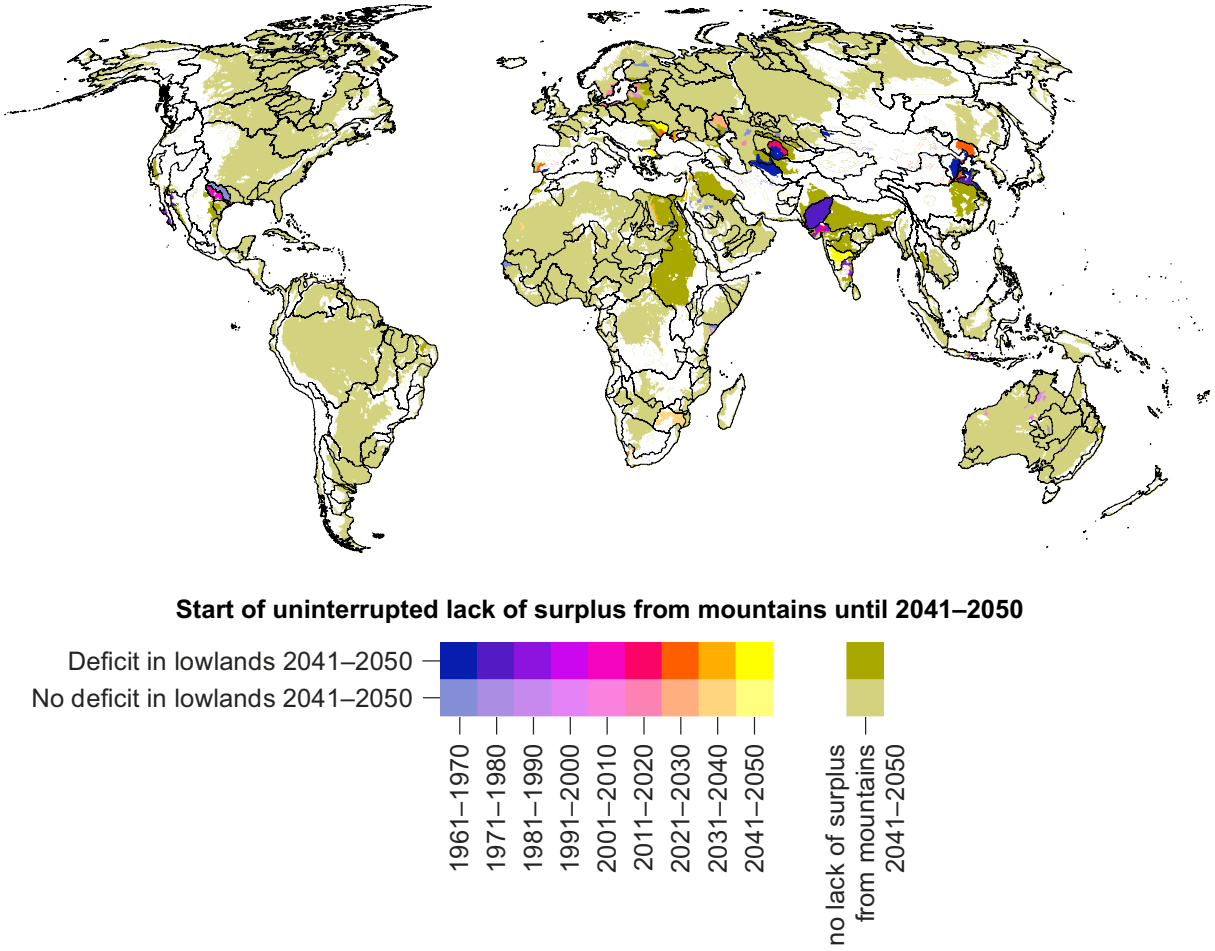

Supplementary Figure S5. Hot spot lowland regions potentially depending on mountain water resources 2041–2050, showing current lowland area equipped for irrigation (a, b) and lowland food production (c, d). Beige denotes areas where mountains as per the definition used here occupy less than 5% of total catchment area, and an assessment from the viewpoint of lowlands should only be done carefully (shown in Supplementary Fig. S10). Results are from the SSP2-RCP6.0 scenario. See also Fig. 3.

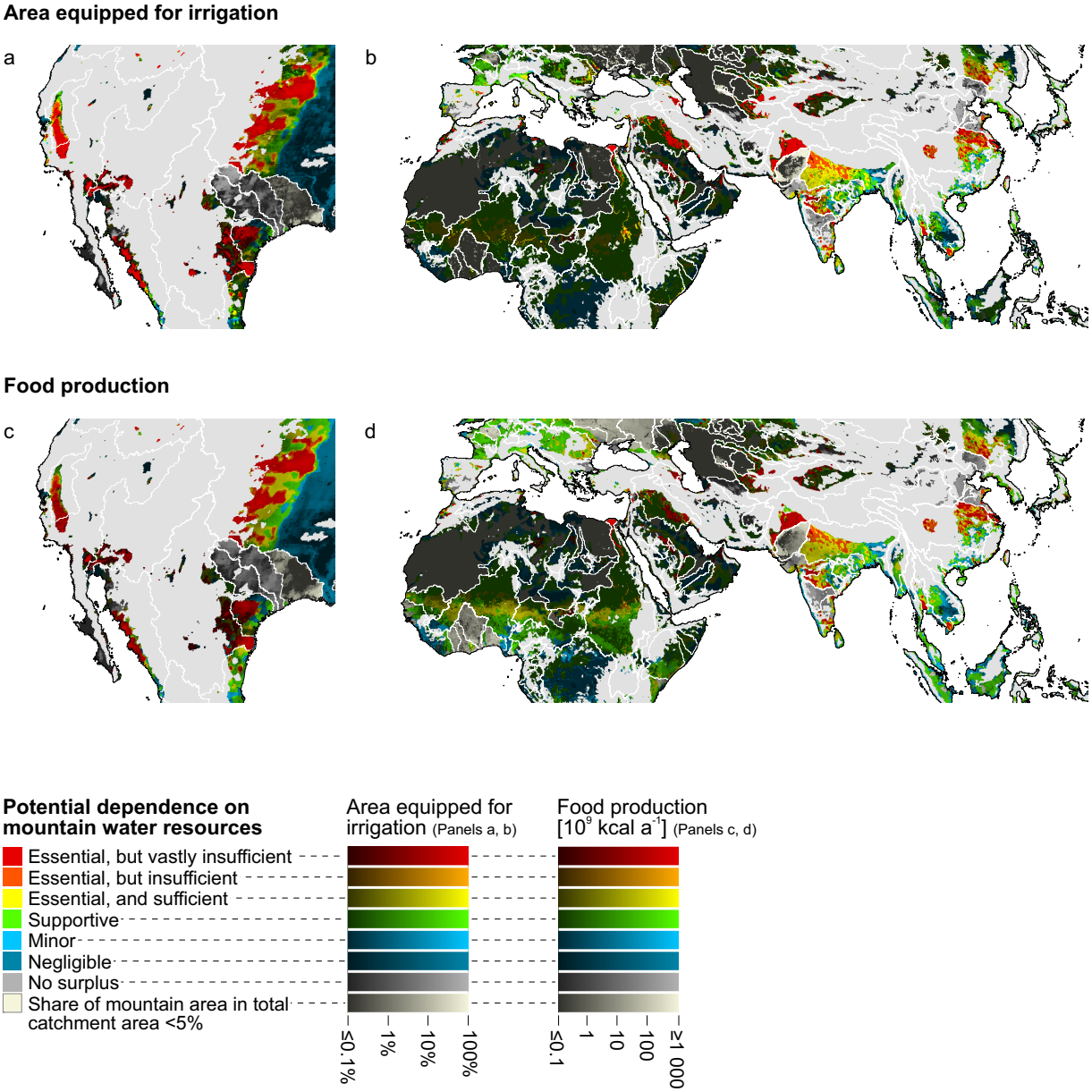

Supplementary Figure S6. Spatial patterns of disproportionality of mountain runoff 1961–2050. Global results are shown for 2001–2010 (a), whereas magnification of selected regions are shown for 1961–1970, 2001–2010 and 2041–2050 (b–g). The boundaries of catchments with an area of 100 000 km² and more are drawn for orientation, and projections refer to the SSP2 RCP6.0 scenario. For temporal evolution by hydrobelt see Supplementary Fig. S7.

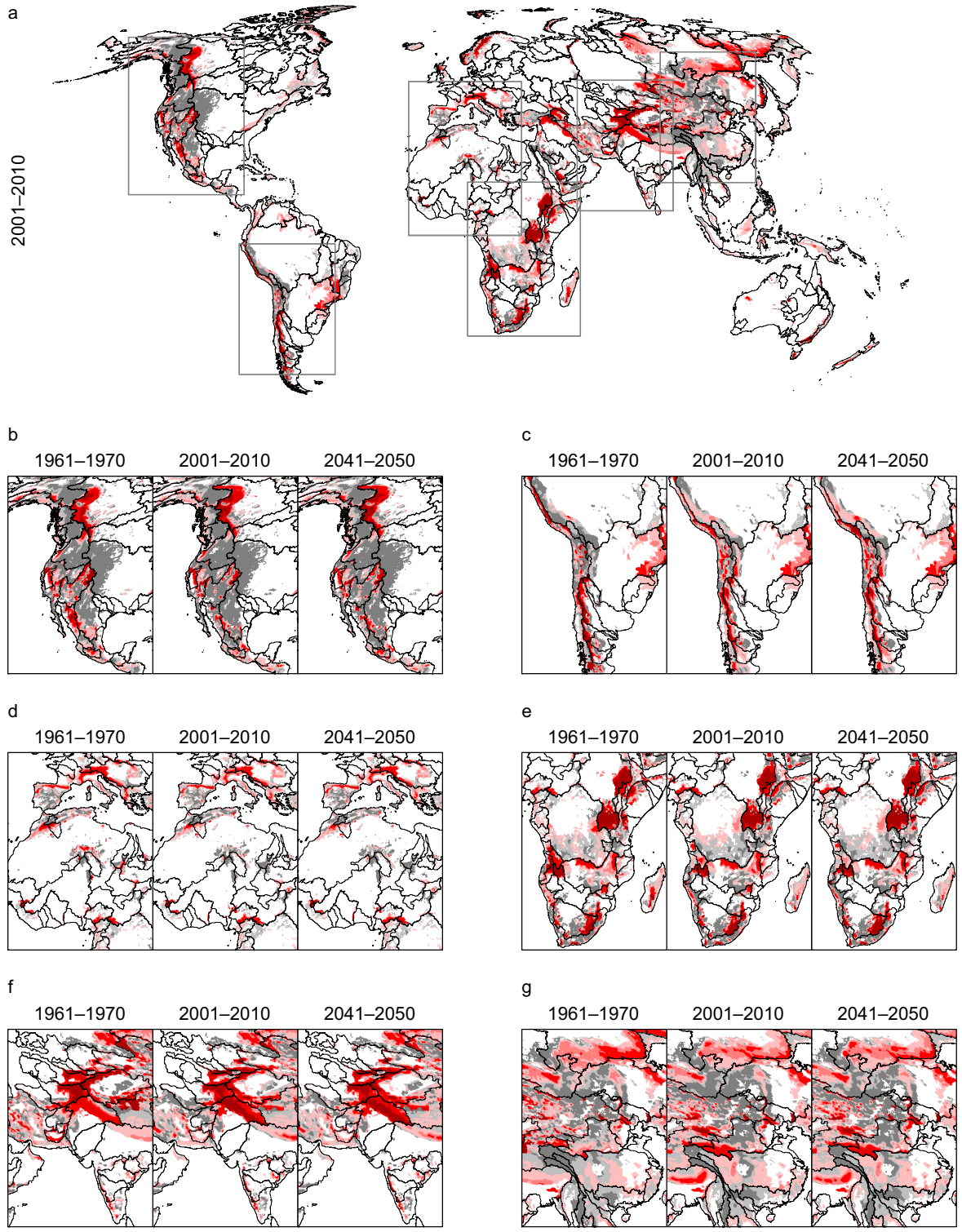

Supplementary Figure S7. Temporal evolution of disproportionality of mountain runoff 1961–2050. Results are shown as decadal averages, summarised for all hydrobelts (a) as well as differentiated by hydrobelt (b–i). Projections refer to the SSP2-RCP6.0 scenario. For spatial patterns see Supplementary Fig. S6.

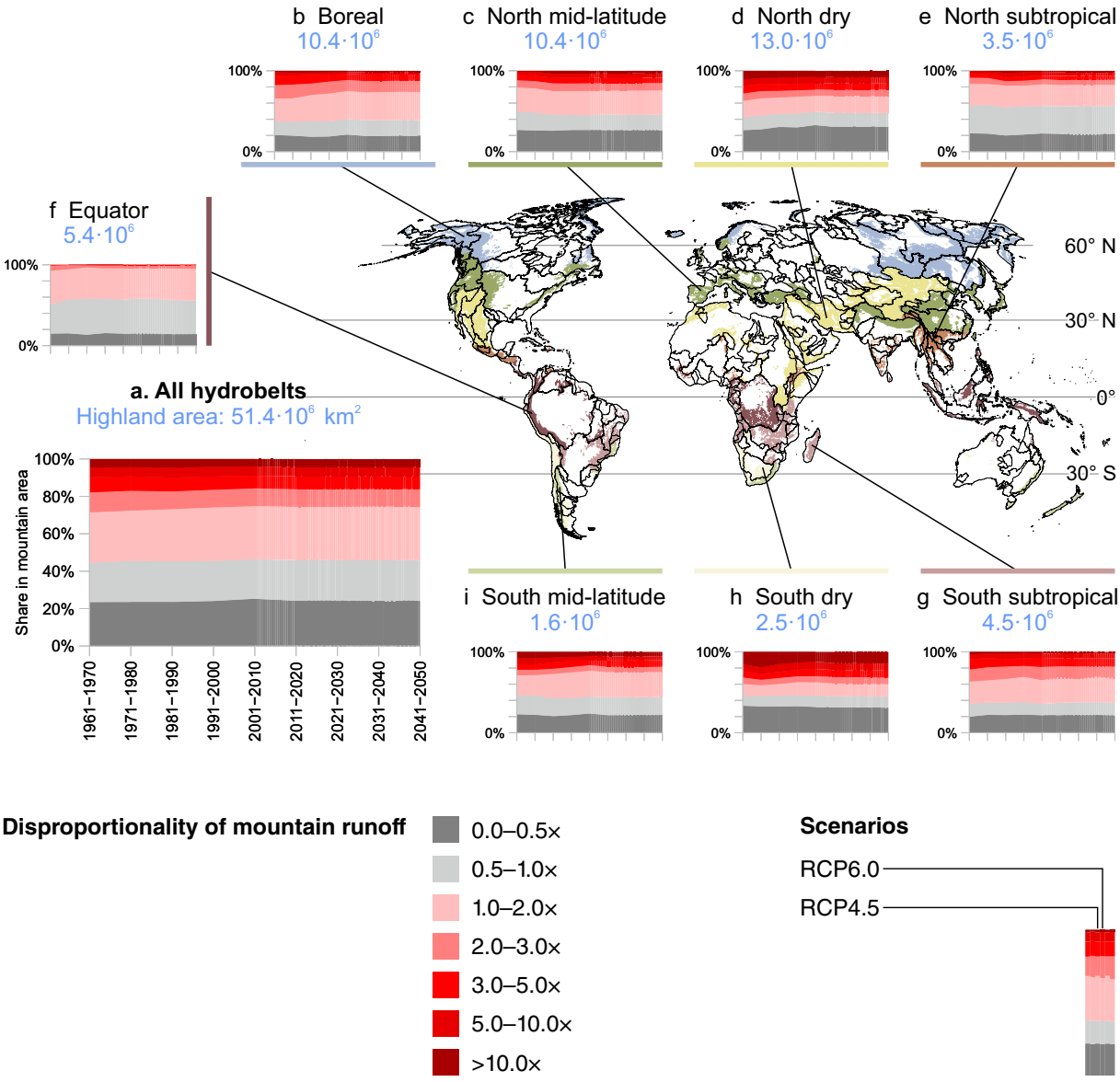

Supplementary Figure S8. Population, total water consumption, per-capita water consumption and runoff 1961–2050. Results are shown individually at decadal scale for mountain and lowland areas (a, d, g, j) as well as differentiated by hydrobelt for mountain (b, e, h, k) and lowland (c, f, i, l) areas.

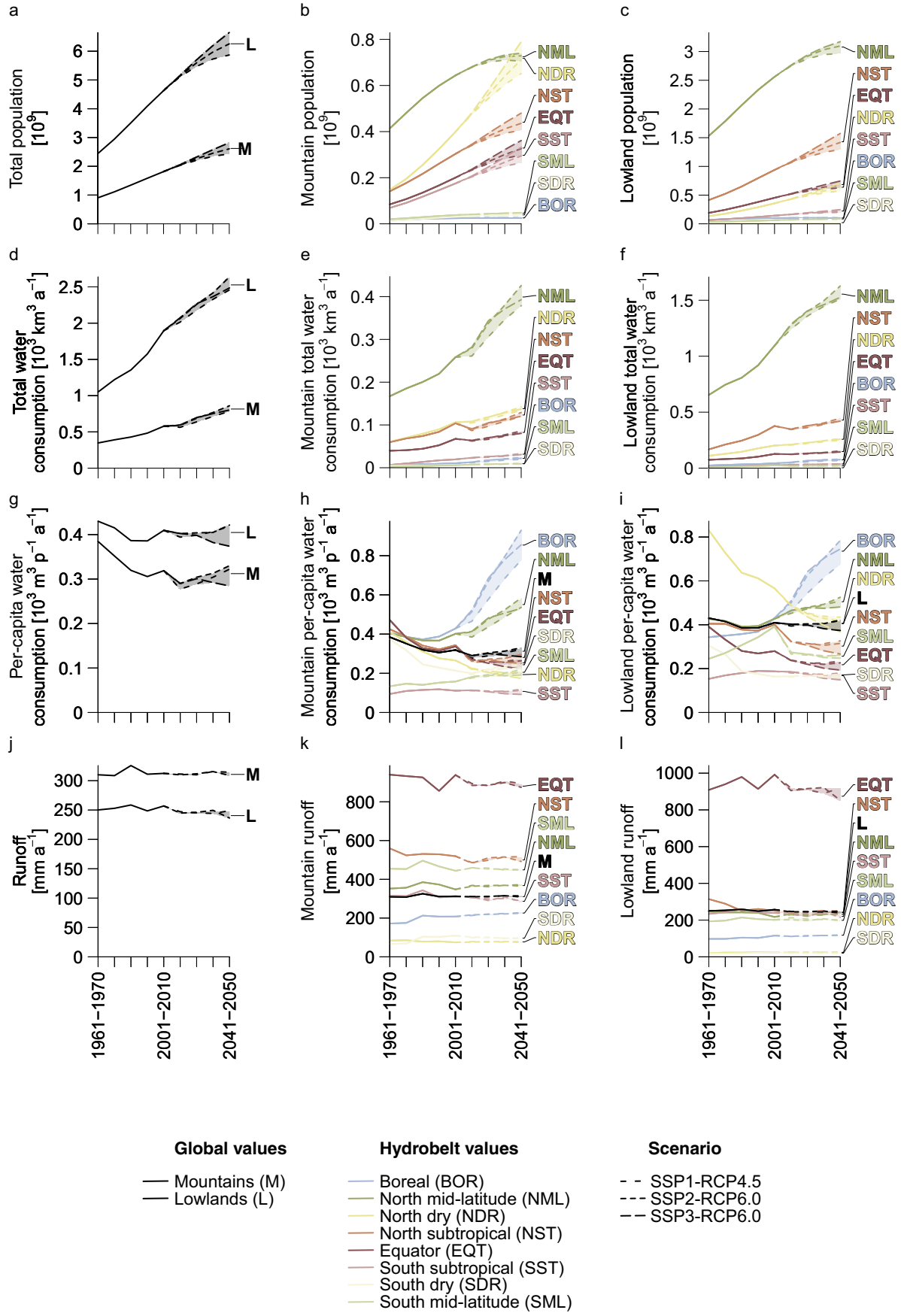

Supplementary Figure S9. Lowland area equipped for irrigation (AEI) under non-sustainable blue water use and dependent on essential mountain runoff contributions in the 2000s and 2040s. For 2041–2050, the SSP2-RCP6.0 scenario was used, and it was assumed that location and extent of AEI are identical to year 2005.

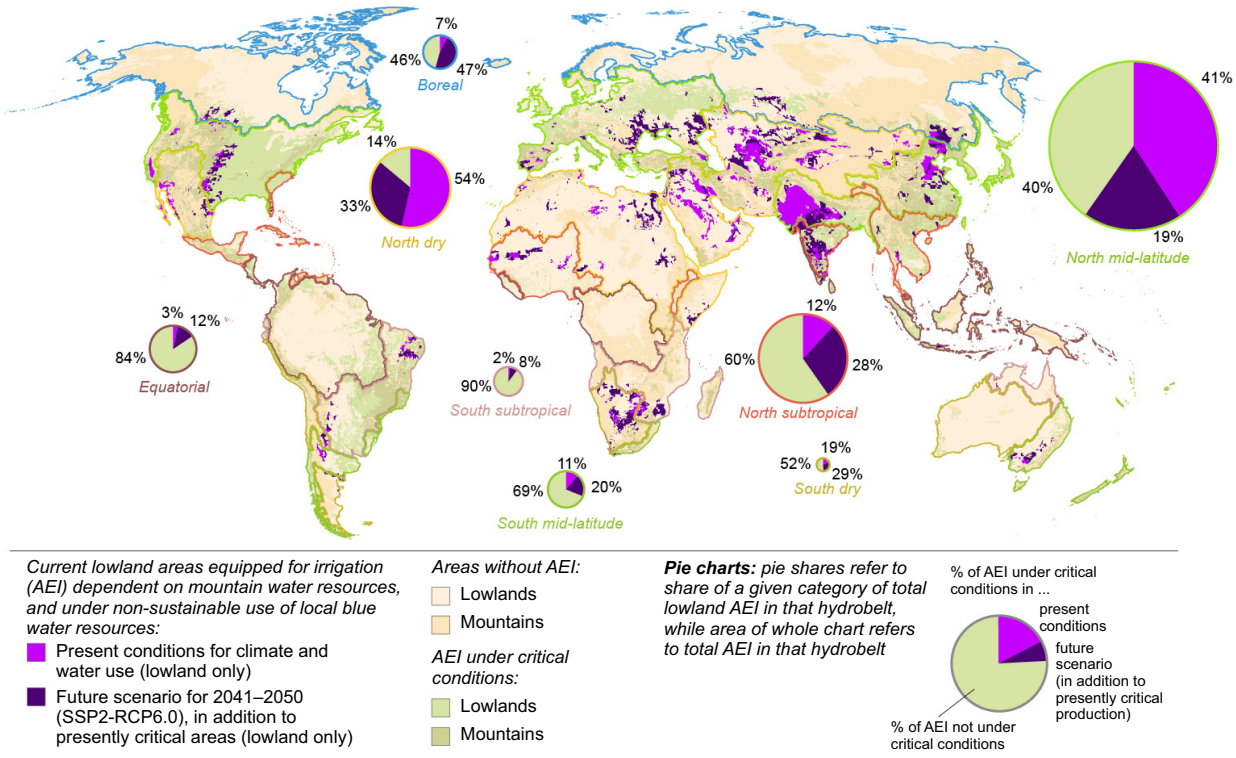

Supplementary Figure S10. Potential dependence on mountain resources 1961–2050, spatial patterns for catchments with a share in mountain area of less than 5%. Results are shown from the viewpoint of lowland areas for the time periods 1961–1970 (a), 2001–2010 (b) and 2041–2050 (c). The boundaries of catchments with an area of 100 000 km² and more are drawn for orientation, and projections refer to the SSP2-RCP6.0 scenario. See also Fig. 3a–c in main article. Since the share of mountains is small, results should be interpreted carefully and bearing in mind mountain contributions to total catchment runoff (cf. Supplementary Fig. S11).

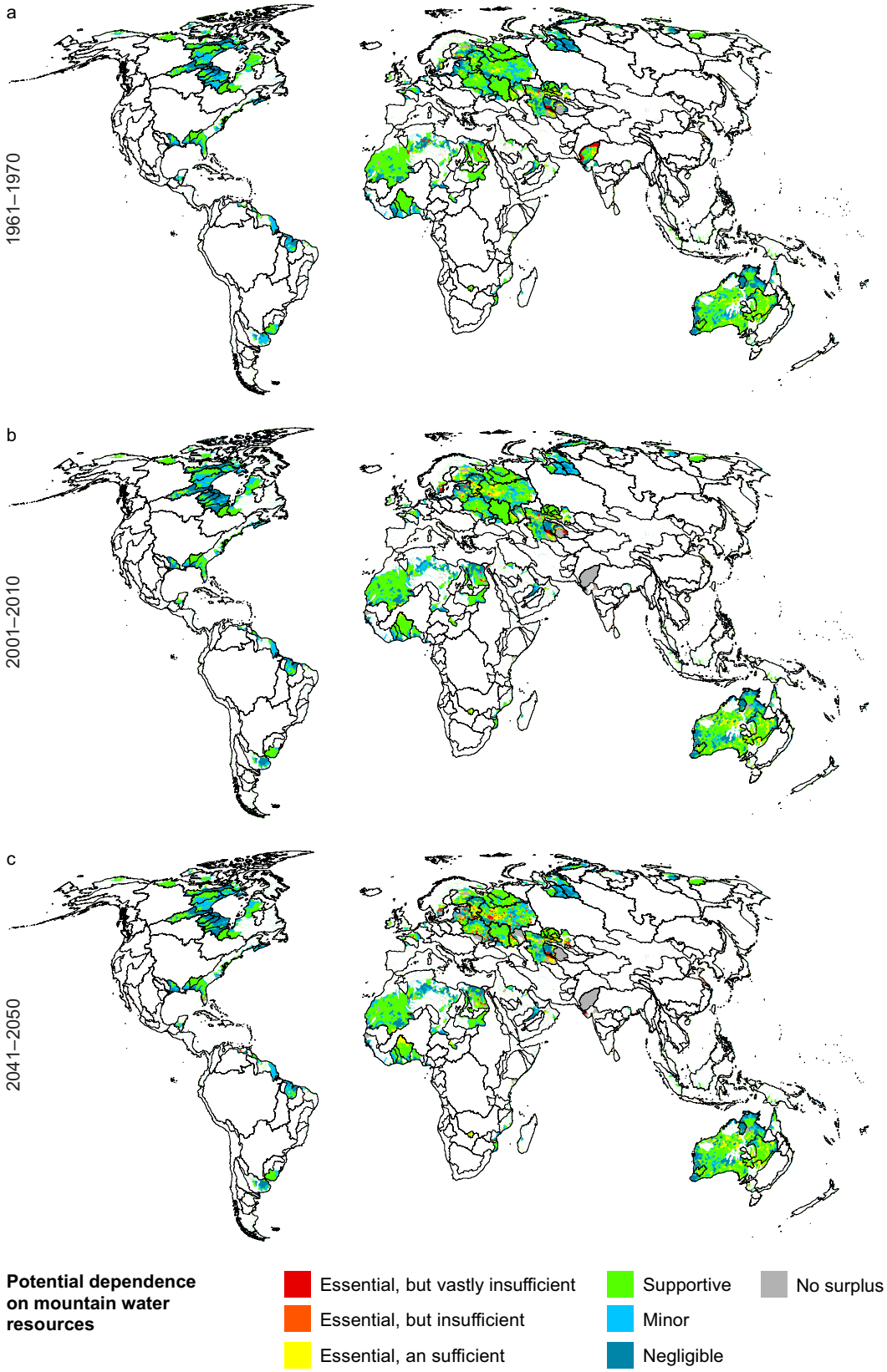

Supplementary Figure S11. Contribution of mountains to total catchment discharge (a) and ratio of mountain share in total catchment discharge to mountain share in total catchment area (b) 2001–2010. In (a), a figure of 100% means that all discharge in a basin originates in its mountain area, and 0% that all discharge originates in its lowland area. In (b), a value of 1 means that mountains contribute as much to total catchment discharge as they do to total catchment area. Values above 1 denote disproportionally high discharge contributions from mountains, values below 1 disproportionally low discharge contributions from mountains. For both computations, results are shown for the time period 2001–2010 only since changes over the timeframe 1961–2050 are small. The boundaries of catchments with an area of 100 000 km² and more are drawn for orientation.

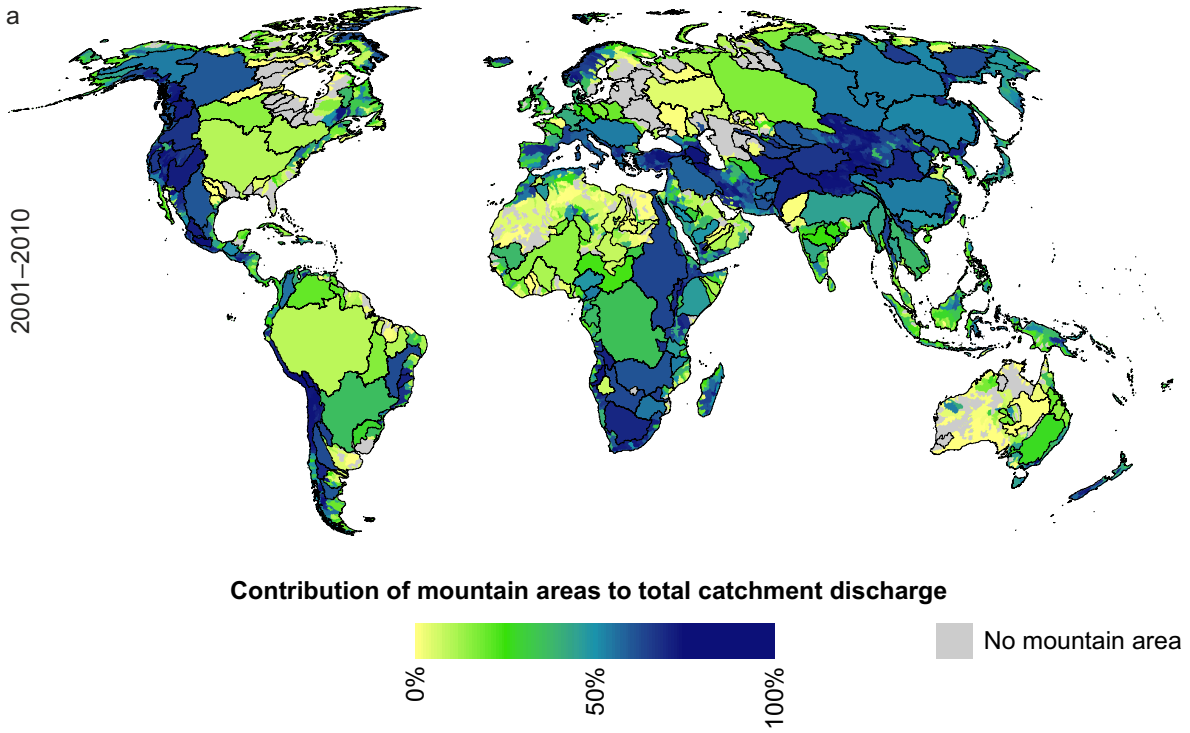

Supplementary Figure S12. Arheic mountain areas 1961–2050. The map shows the number of decades with mean annual runoff of less than 3 mm a^{-1} (see Methods). The boundaries of catchments with an area of 100 000 km² and more are drawn for orientation.

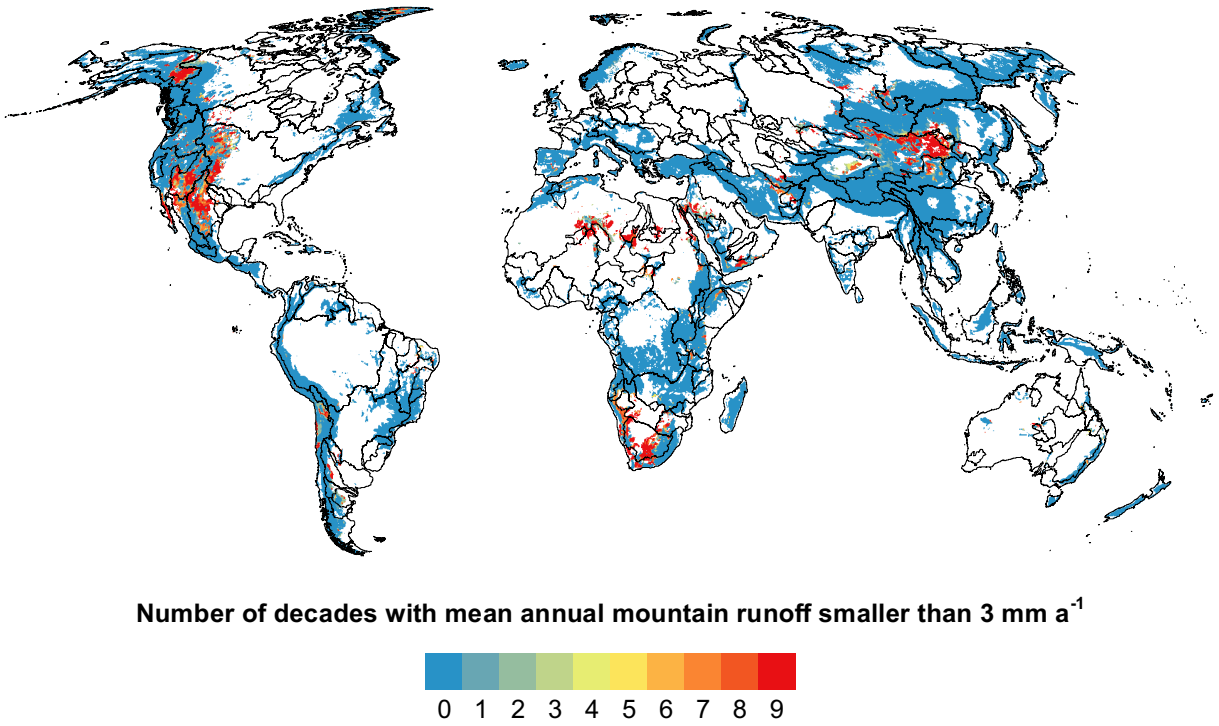

Supplementary Figure S13. Detailed breakdown of drivers causing changes in dependence on mountain water resources 2041–2050. As a baseline, the bottom part of each circular plot represents the number of lowland inhabitants per category 2041–2050, assuming that runoff and total water consumption remain unchanged at 1961–1970 level. The corresponding population numbers are noted under the sectors in Panel a (e.g., 962 M lowland inhabitants potentially depend on essential and sufficient contributions form mountain areas). The top part of the circular plot in Panel a shows results for 2041–2050 under changed conditions as projected with the SSP2-RCP6.0 scenario, and as shown in the main article. Panels b to e then each show results for changes in only one driver, namely mountain runoff (b), mountain water consumption (c), lowland runoff (d), and lowland water consumption (e), all referring to SSP2-RCP6.0. The changes in population per category are noted above each sector for all panels, giving the numbers reported in Table 2 of the main text.

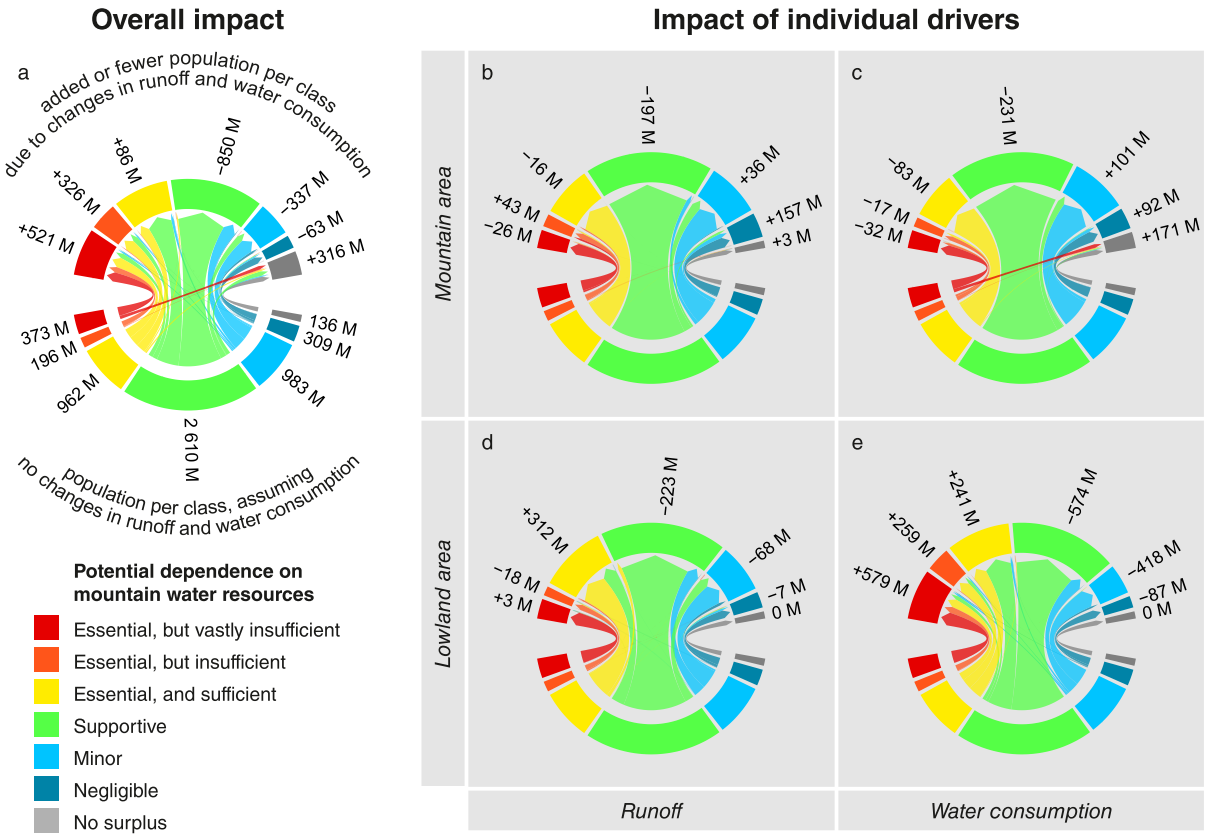

Supplementary Figure S14. Potential dependence on mountain water resources 2041–2050 under alternative scenarios. Results are shown for all three scenarios examined, namely SSP1-RCP4.5 (a), SSP2-RCP6.0 (b) and SSP3-RCP6.0 (c).

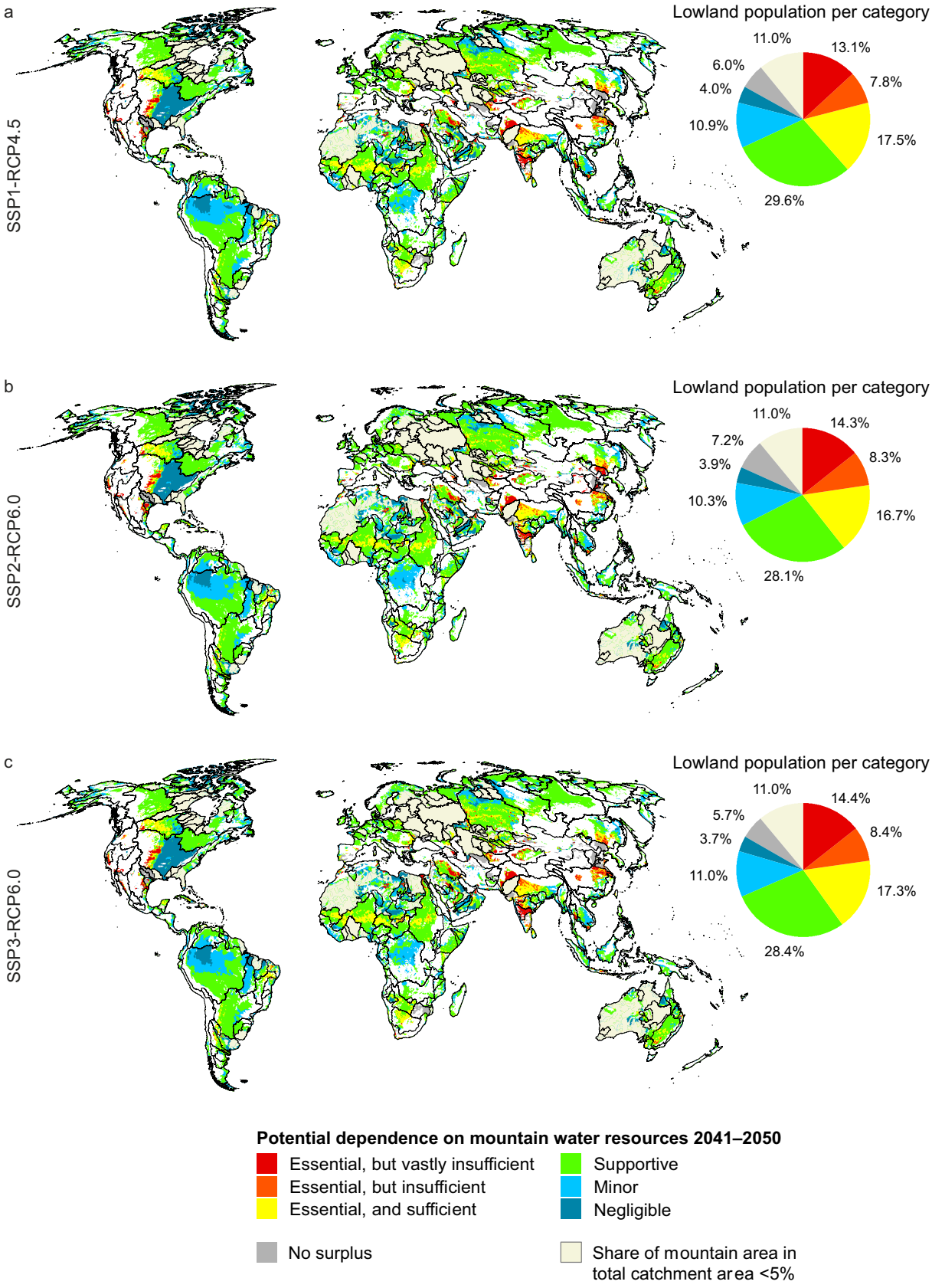

Supplementary Figure S15. Agreement of GCMs on median projected result for dependence on mountain water resources in 2041–2050. Results refer to categories of water resources index ***W*** and are shown for all three scenarios examined, namely SSP1-RCP4.5 (a), SSP2-RCP6.0 (b) and SSP3-RCP6.0 (c).

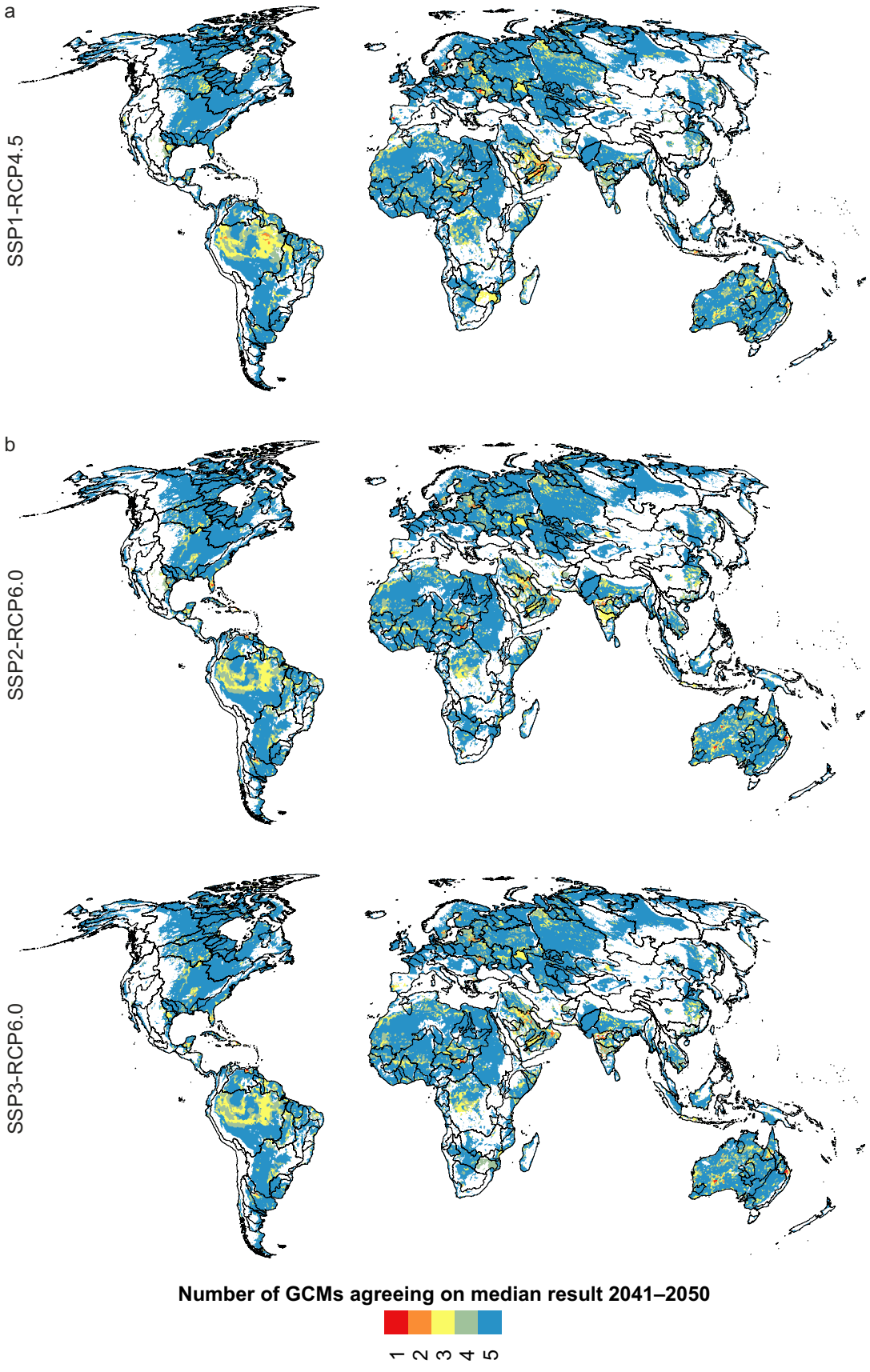

Supplementary Figure S16. Model performance of PCR-GLOBWB run at two different spatial resolutions. The lines show the cumulative frequency distribution of the Kling-Gupta efficiency score[10] below (a) and above (b) 1 000 m a.s.l. Results for 5 arc minutes grid – as used in our study – are in blue, 30 arc minutes grid in green. Reproduced from ref. [2].

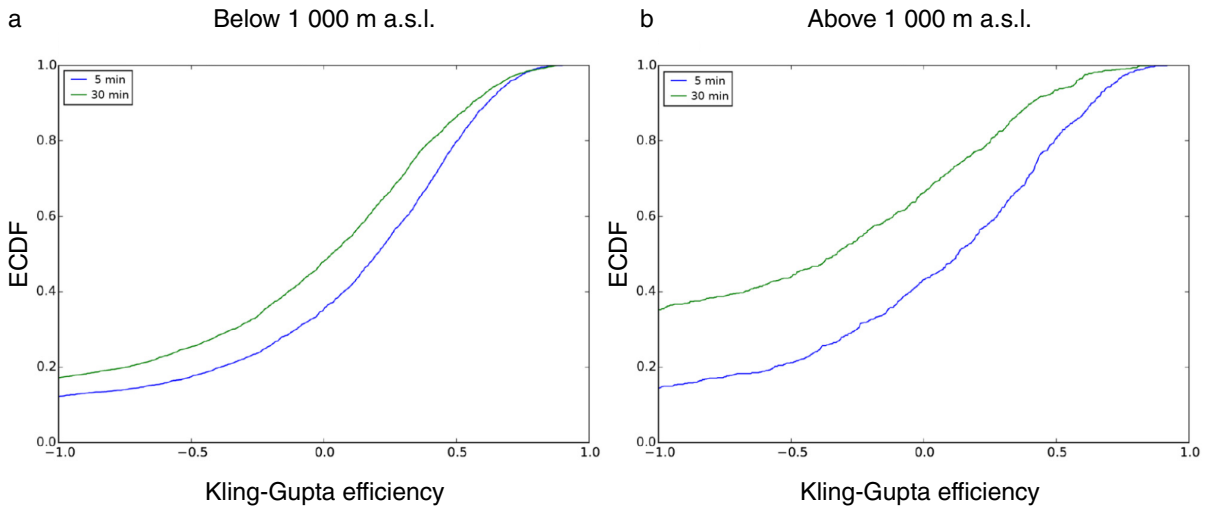

Supplementary Figure S17. Comparison of GSCD long-term mean annual discharge with PCR-GLOBWB 2 mean annual discharge 1961–2010, differentiated by 100 m elevation bands. Results are shown at global scale as well as differentiated by hydrobelts, shares in land surface area are shown for context.

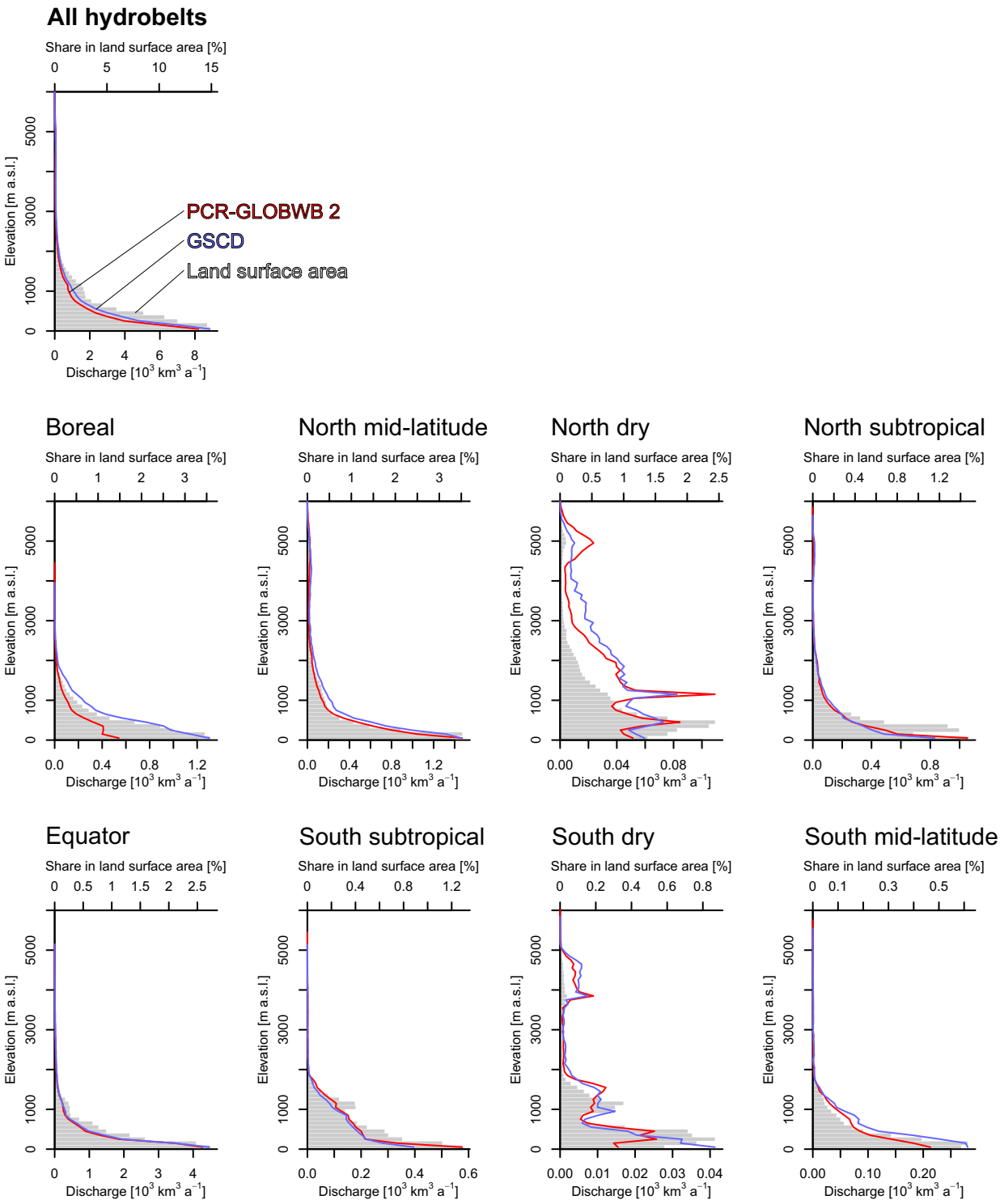

Supplementary Figure S18. Comparison of results obtained with original PCR-GLOBWB 2 outputs and outputs obtained from PCR-GLOBWB 2 adjusted with GSCD. Panel a gives the results of the original PCR-GLOBWB 2 outputs as map and pie chart. In panel b, PCR-GLOBWB 2 runoff was adjusted to fit the long-term behaviour of the Global Streamflow Characteristics Dataset (GSCD) mean annual runoff[1].